The Analysis of Kickpoints in Carbon Fibre Composite Golf Shafts

By

Josh Roberts

A thesis submitted to The University of Birmingham

For the degree of MASTERS OF RESEARCH

School of Metallurgy and Materials

College of Engineering and Physical Sciences

The University of Birmingham

September 2012

Contents

Abstract

The aim of this thesis is to characterise and quantify the construction method of carbon fibre composite golf shafts and the subsequent kickpoint position of the shaft, for the future manufacture and testing of shafts with specific kickpoints. For this purpose the geometrical and material properties of commercial carbon fibre composite golf shafts were investigated for their influence on the kickpoint position. The shafts were investigated via geometrical, static deflection tests, quasi – static frequency and material analysis.

The static stiffness of the commercial shafts ranged between 242.1 – 563.3 N/m at a single cantilever length. The kickpoint position in commercial golf shafts ranges from 45 – 52.9 % of the shaft length and the position of the kickpoint is the location of the greatest strain in static testing (1700 μm). The kickpoint position decreased as the gradient of the stiffness profile of the shaft increased ($R^2 = 0.77$).

The quasi – static frequency analysis presented a maximum 4.8 % variation around the circumference of sheet laminated shafts and 0.2 % variation in filament wound shafts, the variation around the circumference of the sheet laminated shafts is the result of "seams" due to resin rich regions in the manufacturing process resulting in a drop of volume fraction from the mean of 8.9 % and local wall thickness variation around the circumference (6 %).

The size of the resin rich regions in the sheet laminated shafts were the result of off-axis fibre orientations between plies constraining fibre movement during the cure cycle. Though the "seam" position had a measurable effect on the stiffness of the shaft, a negligible influence of "seam" orientation on kickpoint position was analysed.

Acknowledgements

I would like to say thank you to my lead supervisor Dr Martin Strangwood, who gave constant feedback, guidance, advice and encouragement during this MRes but also throughout my Undergraduate degree too. The skills and knowledge gained throughout my time at The University of Birmingham will be critical to my future career. Thank you is also required for my industry supervisor Dr Steve Otto, who always brought a fresh pair of eyes with continued ideas and input into the research.

The experimental work would not have been possible without the support of the lab technician Mick Cunningham, from my first day as a Undergraduate to my last day as a Postgraduate he went out of his way to support you by any means possible. A thank you to all of my colleagues in the office, though an extended thank you must go to Carl Slater for his advice during my thesis.

The biggest thank you goes to my family, who without their support to attend The University of Birmingham as an undergraduate and stay on for postgraduate studies would not have been possible. This thesis is dedicated to them for everything they have provided me with for the past 5 years.

1. Introduction

1.1. History of the Golf Shaft

The manufacturing of golf clubs between the 17th through to the 19th century in Great Britain relied on materials indigenous to the manufactures region, typically these materials for the shafts were hardwoods (Dangawood, ash, lemonwood and lancewood). The golfer chose their shaft wood from the "feel" that they received to their own preference. The early 19th century saw the introduction of hickory as a shaft material, hickory had a low density, high modulus, durability and resistance to warping compared to other hardwood shafts. Although one disadvantage of the hardwood shafts is that their low strength lead to damaged and broken shafts, once a shaft is broken it was extremely difficult to find a shaft to duplicate the "feel" from the previous shaft.

The late 19th century the development of shaft technology prompting the use of metallic alloys as shaft materials, although this technology was not fully utilised until the early 20th century with the production of the hollow metal shaft. The manufacturing method of the hollow metal shaft allowed variables such as taper, wall thickness and diameter to be altered, thus allowing the engineering of various stiffness and kickpoint position for a shaft.

Composite materials were introduced to the golf shaft in the 1950's with glass fibre shafts, the utilisation of these materials resulted in reduced weight and no compromise of strength compared to the steel shafts. However, by the early 1970's glass fibre shafts were phased out as a result of poor torsional stiffness and poor tensile strength. The carbon fibre composite shafts ("graphite" shafts) were produced in the late 1960's resulting in the phasing out of the glass fibre shafts due to their increased tensile strength. The carbon fibre shafts "boomed" in the early 1970's and has been mass produced since.

1.2. The Role of the Golf Club Shaft

The role of the shaft is pivotal in the golf swing in delivering the club head to the ball for a range of shots and club types from drivers to putters. The shaft has a club head attached with mass ranges of 180 – 350 g and will be subjected to swing speeds of 2.2 – 62.6 ms^{-1} (Strangwood, 2003). The dynamic swing motions, range of head masses and swing speeds will result in significant deformation as a result of stresses and torques during the golf swing.

The analysis of the shaft during the swing has been performed by numerous authors (Milne & Davis, 1992; Horwood, 1994; Newman, Clay & Strickland, 1997; Mather and Jowett, 2000; Penner, 2003). At the initiation of the downswing, the golf club is subjected to the torque exerted by the golfer and the inertia of the golf club head resulting in the shaft being bent backwards in the plane of swing, as the down swing continues, the shaft straightens out in the plane of swing prior to impact, Figure. 1.1, (Penner, 2003). The recovery of the shaft is a result of the material properties of the shaft, centrifugal and inertial forces placed on the shaft (Horwood, 1994). The deformation to the shaft during the swing has been characterised as the constant transformation of kinetic and strain energy and vice versa (Newman, Clay & Strickland, 1997).

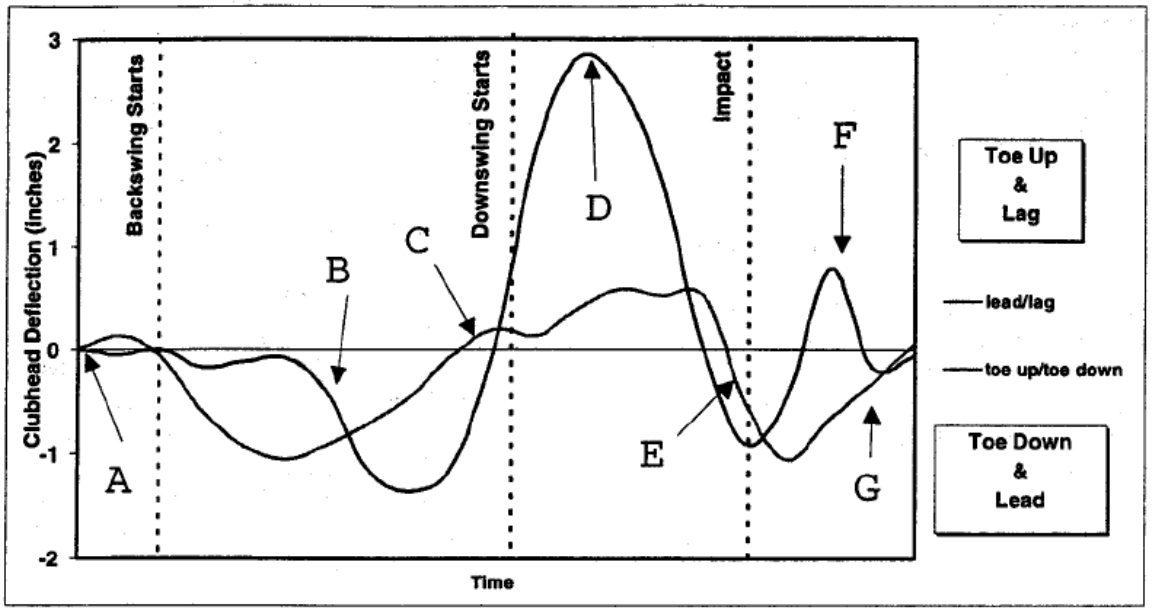

Figure 1.1. The bending of a golf shaft during dynamic swing, the club head leads on the backswing (A & B) and on the downswing presents significant lag (D), on impact the club head leads (E) (Newman, Clay & Strickland, 1997).

The shaft is not subjected just to deformation in the swing phase (lead/lag) but also in the perpendicular plane (toe-up/down) of swing, Figure 1.1. The reason for the bending in the perpendicular plane of swing is said to be the result of the offset centre of gravity of the club head with respect to the shaft centre line. During the dynamic swing, the offset centre of gravity results in a bending moment as the centrifugal force is acting at this position, while a centripetal force is applied via the shaft (Horwood, 1994; Mather and Jowett, 2000), Figure 1.2.

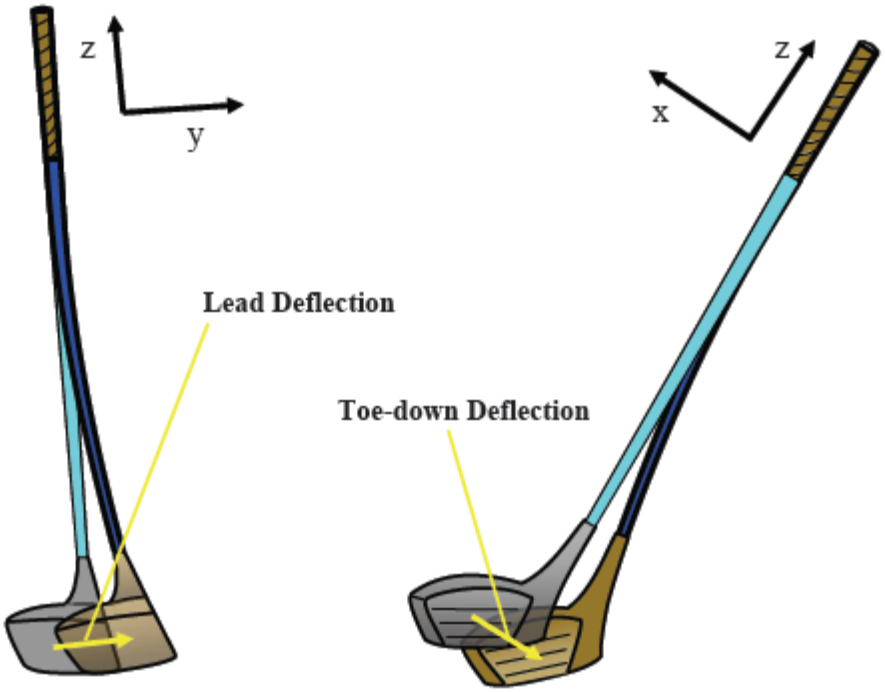

ff

Figure 1.2. Diagram of the deformation of the shaft in the swing phase and perpendicular to the swing phase as a result of the offset centre of gravity of the club head from the shaft centre line (Mackenzie, 2005).

The role of the shaft during impact is said to be minimal due to negligible deflection of the shaft during impact and short impact duration, the shaft had significant deflection prior to impact though this had no effect on dynamic loft (Mather and Jowett, 2000). The shaft does show large vibrations after impact, though the golfer cannot use this information (termed the "feel" of the shot) to influence the shot it will have a psychology on the subsequent shot (Horwood, 1994).

1.3. Properties of the golf club shaft and their assessment

1.3.1. Bending stiffness

The static bending stiffness of a shaft can be measured by simple bending tests on a deflection board, the shaft is gripped at the end and a load is placed at the tip end of the shaft and the deflection measured (Howell, 1992). A second method is the repeated bending test where a stiffness profile along the length of the shaft is generated and takes into account dimensional alterations of the shaft (Brouillette, 2002). Lastly, the third method is the application of a frequency analyser to which the shaft is gripped at the grip end and a mass of 205 g attached to the tip end to analyse the fundamental frequency.

The bending stiffness of a golf shaft is categorised by the shaft manufacture in relative categories ranging from ladies flex to stiff flex, though it should be noted that there are no standards set between manufactures for these relative stiffness categories (Horwood, 1995). Work performed by Summitt (2000) on the deflection of stiff and ladies flex shafts at a single cantilever length of 1.05 m produced deflection value ranges of 0.09 – 0.13 m and 0.11 – 0.15 m respectively, the overlap of the deflection ranges between the stiff and ladies flex shaft is a result of no standards set for stiffness categories (Horwood, 1995).

The bending stiffness of a shaft could influence the club head speed of a shaft because, during the down swing, the shaft bends and stores strain energy, later in the down swing this strain energy is converted to kinetic energy to potentially increase club head speed by the addition of kick velocity (Butler & Winfield, 1994). Milne and Davis (1992) produced a 2D model of the "in swing plane" and showed shaft deflection of 10 cm, though the authors cited that bending stiffness of the shaft has negligible influence on the dynamics of the swing. Critically, Milne and Davis (1992) did not include the influence of kick velocity which

research has shown to be 5% of the club head speed (Horwood, 1994) and a 2D model does not depict the 3D deformation of the shaft, though research by Butler & Winfield (1994) found that deformation in the longitudinal axis (out of swing plane) has negligible influence on club head speed.

The role of bending stiffness on club head speed has been investigated further by simulation studies by MacKenzie (2009), the author used a three dimensional model of the dynamic swing and included the upper body in the model to produce optimised swing conditions for the shaft conditions used. The results of the authors work showed that club head speed of the shaft did alter more than 0.1 ms^{-1} with shaft stiffness, thus shaft stiffness has negligible influence on club head speed. The work by Mackenzie is supported by Betzler (2010) with experimental data from experienced players using three stiffness variations of shaft, Table 1.1. The model by MacKenzie (2009) assumes optimal swing conditions of the golfer, though research has shown that varying shaft stiffness alters wrist kinematics (Betzler, 2010) and shoulder angular kinematics (Wallace and Hubbell, 2001). It is not known whether a golfer can adapt to that degree or the time this would take.

Table 1.1. Data from both McKenzie (2009) and Betzler (2010) show no influence of bending stiffness of a shaft on the club head speed in optimised swing models.

	McKenzie (2009)		**Betzler (2010)**	
	Club head Speed (m/s)	**Standard Deviation**	**Club head Speed (m/s)**	**Standard Deviation**
L - flex	44.96	N/A	45.8	2.57
R - flex	45.01	N/A	46	2.51
X - flex	45.04	N/A	45.7	2.4

Stanbridge, Jones & Mitchell (2004) who investigated the drive distance achieved by varying the shaft stiffness (232, 267 and 324 CPM) on 30 junior male golfers with seven irons showed that variations in stiffness did not affect driving distance. However, when the results were investigated on an individual basis 21 of 30 participants had their greatest driving distance with specific shaft stiffness, Figure 1.3, thus shaft properties may be matched to specific golfers for increased performance. This work has been supported by Worobets and Stefanyshyn (2008) who found that for 12 out 21 golfers shaft stiffness had no influence on impact velocity, though the golfers achieved their maximum impact velocity with various stiffness shafts.

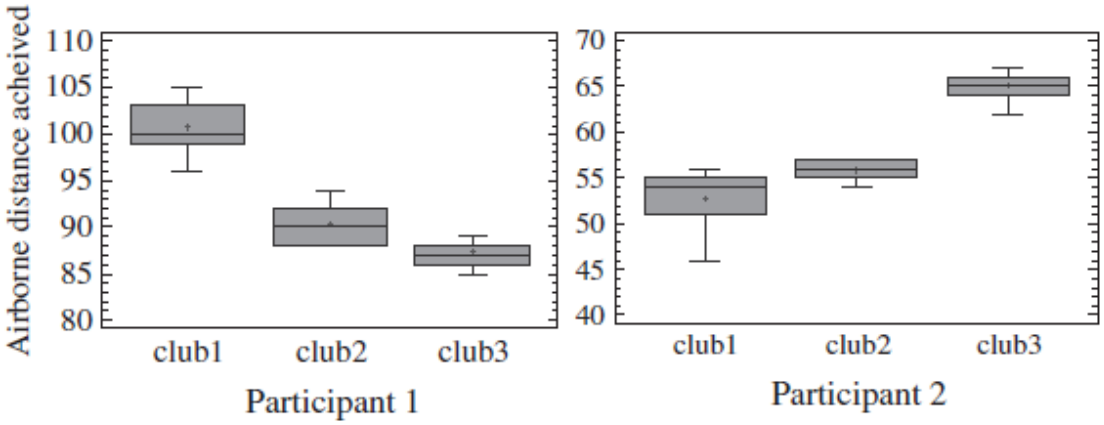

Figure 1.3. Data of the airborne distance achieved for two participants, club 1 -3 have a frequency of 324, 267 and 232 CPM respectively and both participants achieved greater distance with specific shaft stiffness.

Bending stiffness can influence the dynamic loft via the stiffness of the shaft affecting the forward bending of the shaft, thus a less stiff shaft will be subject to a greater degree of forward bending resulting in increased dynamic loft (Maltby, 1995). Mather and Cooper (1994) showed that a lead deflection of 5 cm during the swing prior to impact can result in a

5^{o} increase in dynamic loft. Mackenzie (2005) supported the findings of Mather and Cooper (1994) in shaft stiffness affecting dynamic loft in an optimised three dimensional model, each increment of 1 cm lead deflection, resulted in a 0.8^{o} increase in dynamic loft. However further research in the area has shown that alterations in shaft bending stiffness results in negligible variation of dynamic loft, Tsujiuchi, Koizumi & Tomii (2002) performed a three subject experimental study and found no influence on dynamic loft angle. Betzler (2010) performed an experimental test on launch conditions with respect to shaft stiffness on experienced golfers and found no relationship between shaft stiffness and launch conditions. The modelling work by Mather and Cooper (1994) and Mackenzie (2005) represents optimum swing conditions as stated earlier, thus why the experimental research (Tsujiuchi, Koizumi & Tomii, 2002; Betzler, 2010) showed negligible alterations of dynamic loft with shaft stiffness as a result of a golfer adapting to a new shaft but not to the degree of an optimised swing in the proposed models.

1.3.2. Torsional stiffness

The torsional stiffness of a shaft is assessed by clamping the grip end of the shaft, the tip end of the shaft has a lever arm attached with a known mass placed on the lever arm and the subsequent twist of the shaft is measured, the torsional stiffness is expressed by Equation 1.1.

Equation 1.1.

$$Torsional\ Stiffness = {}^{57.3\ m\ g\ L}/_{\theta}$$

Where: m is the mass attached (kg)

g is gravity (ms^{-2})

L is the lever arm length (m)

Θ is the angle of deviation for the lever arm (^{o})

The shaft during the dynamic swing is subjected to a twisting motion as a result of the centre of gravity of the club being in the head and offset from the centre line of the shaft. Torsional stiffness of the shaft is required to prevent the head leading or lagging behind the shaft causing the head to not address the ball correctly at impact (sliced or hooked shot) (Horwood, 1994; Strangwood, 2003). Research by Kojima and Hori (1995) on the influence of torsional stiffness on ball velocity and how the club head addresses the ball, (the authors used two shafts of high and low torsional stiffness on a golf robot) showed that a shaft with higher torsional produced increased ball velocity and addressed the ball correctly producing consistent ball trajectories. Though the work by Kojima and Hori was not performed on human swings and thus does not include any adaptations that may occur, therefore, the results may not be transferrable.

1.3.3. Kickpoint

Kickpoint may also be defined as the bend point or flex point depending on the author. The kickpoint of a shaft can be assessed by three approaches; the first, is clamping the butt end of

the shaft and placing a load on the tip end of the shaft, a imaginary straight line is drawn between the clamped butt end and tip end and the kickpoint is the position along the shafts length at the greatest deviation from the straight line, it can also be expressed as the smallest radius of curvature (Huntley, 2007). The second approach is tested in a similar fashion to that of the first approach, except the tip is clamped and the butt end of the shaft has a load placed. The third approach is to test the shaft in a compression test to make the shaft buckle, the kickpoint is measured in the same fashion as the first approach and expressed as percentage distance of the length away from the tip end (Cheong, 2005).

Research by Chou & Roberts (1994) found variations in the kickpoint results produced for the three testing methods outlined above. The first method resulted in kickpoint results at a greater distance from the tip end of the shaft compared to the other two methods, this is a result of the bending moment of the shaft being greatest nearer the clamp, thus resulting in the kickpoint being a greater distance from the tip. The same reasoning can be applied to the second method resulting in a kickpoint closer to the tip of the shaft. The variation in results can be attributed to the first and second methods having a section of the shaft clamped (does not act), however the third method results in the whole shaft acting.

Two shafts tested on a deflection board may have the same bending stiffness though their kickpoint position will vary; this is a result of the stiffness profile along the length of the shaft, a shaft can be tip stiff resulting in a high kickpoint or butt stiff resulting in a low kickpoint (Strangwood, 2003). The stiffness profile of the shafts is a result of the dimensions, wall thickness and material properties of the shaft (Huntley, 2007). The range of kick points in the modern day shafts range from 40 – 60 % (Cheong, 2005; Huntley, 2007).

The position of the kickpoint along the length of the shaft varies the dynamic loft of the ball, a low kickpoint producing decreased dynamic loft (Milne, 1990), Figure 1.4. While research

provided by Chou & Roberts (1994) found that alterations of kickpoint in the golf shaft provided inconsistent dynamic loft results produced by a golf swing robot. However, the authors used only three composite shafts which have a range of frequency (267 – 281 CPM), torque (2.4 – 4.4 deg) which could influence dynamic loft, while the three shafts used in this study had a small range of kickpoint (40.4 – 48.5 %) compared to the range in manufacture of 40 – 60% (Cheong, 2005; Huntley, 2007).

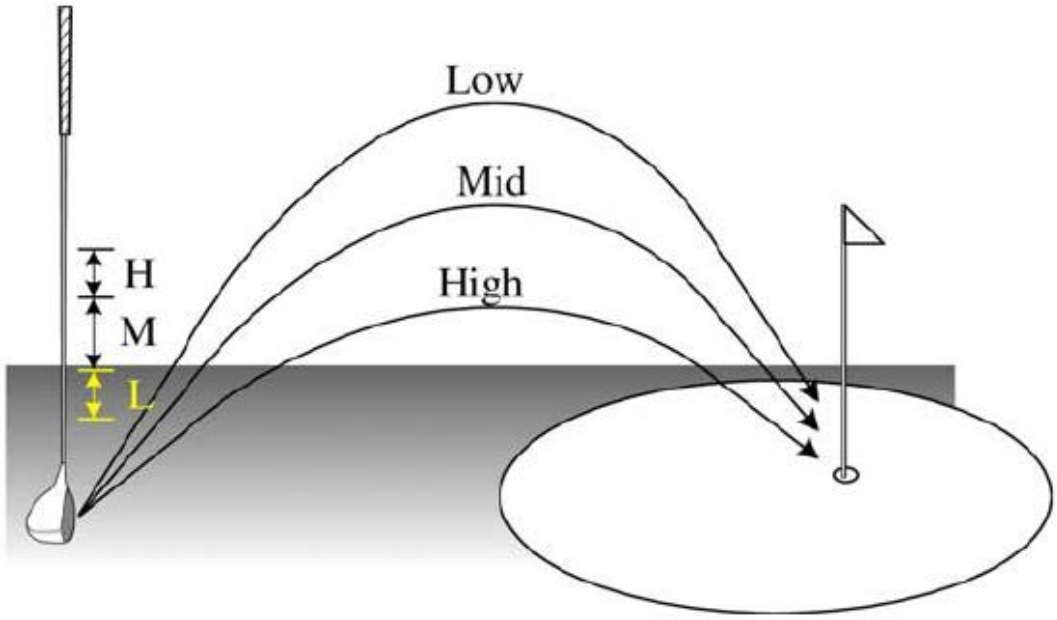

Figure 1.4. Diagram depicting the position of the kickpoint affecting the dynamic loft angle (Cheong et al, 2005).

1.3.4. Mass

The mass range for a typical golf shaft is a range of 59 to 110 g (Howell, 1992). Research performed by swing models on the effect of shaft mass has shown that decreasing the shaft mass from 120 to 50 g under optimum operating conditions results in a 3.3 yard increase in drive distance and a 2 % increase in club head speed (Werner & Greig, 2001), the increase in

drive distance originates from an increased impact velocity (Chen, Inoue & Shibata, 2005). The above authors suggest that the optimum golf shaft should be as light as possible, though shaft mass provides proprioceptive feedback which is required to produce a consistent swing (Butler & Winfield, 1995).

1.3.5. Dimensions

The dimensions of a golf club shaft consist of shaft diameter, wall thickness and the degree of taper (unless parallel sided). Research by Huntley (2007) on the dimensions of golf club shafts found the diameter of a typical tapered shaft ranged from 8.2 – 8.9 mm at the tip end and 14.8 -15.7 mm at the butt, however the shafts had a reinforced tip section and grip section of a constant diameter. The "stiff" and "regular" flex shafts analysed showed greater diameter at the grip section compared to "ladies" flex as a result of greater mean grip aperture of male players. The mean wall thickness of the analysed golf club shafts by Huntley (2007) presented a mean wall thickness of 0.7 – 1.1 mm, though the reinforced tip section of the shaft had a greater mean wall thickness. The shafts typically showed a constant mean wall thickness from the butt end to the tip section, in some shafts analysed the mean wall thickness decreased between the tip and butt sections.

1.3.6. Length

The length of a golf club is limited to 1.219 m (The R&A, 2008), this length is defined as "the distance from the cap of the grip to the intersection of the shaft centre line with the club sole resting on the ground".

The effect of the length of the shaft on the bending stiffness is expressed by Equation 1.2. The bending stiffness of shafts not tested under a single cantilever length presented

significant overlap of stiffness ranges represented by the manufactures flex rating, though when the shafts were tested again at a single cantilever length, the majority of shafts produced a bending stiffness value that fell within their manufactures flex rating (Huntley, 2007; Summitt, 2000).

Equation 1.2.

$$EI = {}^{F\,L^3}/_{3\,\delta}$$

Where: E is the average shaft elastic modulus (N/m^2)

I is the average second moment of area (m^4)

F is the force applied to the shaft (N)

L is the cantilever length of the shaft (m)

δ is the deflection of the shaft (m)

The influence of shaft length on the dynamic swing of a golfer has been modelled and tested experimentally. The modelling performed by Chen et al. (2005) showed that varying club length relative to arm length (1.5 – 2 times) resulted in increased club head speed prior to impact. Experimental testing on players of varying ability using club lengths ranging from 46 – 52" found that increasing the club length produced increased ball velocity (Wallace, Otto & Nevill, 2007). A model by Werner and Greig (2001) on the influence of shaft length stated that the optimum shaft length would be 1.27 m for increased club head velocity while maintaining accuracy from the shot.

1.4. Manufacturing routes of golf club shafts

1.4.1. Composite Materials and their properties

Composite shafts are generally made from either CFRP (carbon fibre reinforced polymer) or GFRP (glass fibre reinforced polymer) and their production methods will be explain in the latter section. Composite materials are chosen for driver shafts compared to metallic alloys as a result of their lower density, increased modulus and tensile strength (Strangwood, 2003), Table 1.2.

Table1.2. Typical property values for selected shaft materials, the range of values for metallic alloys is a consequence on processing and heat treatment (Strangwood, 2003).

Component	Density (g/cm^3)	Young's modulus parallel to fibres (GPa)	Young's modulus normal to fibres (GPa)	Tensile strength (Mpa)
C-Mn (mild) steel	7.85	210	-	400 - 500
Al-Cu	2.77	73	-	185 - 485
Ti-6 Al-4 V	4.43	110 - 125	-	900 - 1170
HM carbon fibre	1.95	380	12	2400
HS carbon fibre	1.75	230	20	3400
E glass fibre	2.56	76	76	2000
S glass fibre	2.48	86	86	4600

The composites are constructed from continuous fibres embedded within a matrix (epoxy resin), the matrix is necessary for load transfer to the fibres and to protect the fibres from surface attack. The composite has two main arrangements of the continuous fibres in the

matrix, namely unidirectional (fibres run parallel to one another) and two - dimensional weave / twill (fibres woven at 90^{o} in bundles to one another). The unidirectional fibre composite has anisotropic properties in that the modulus parallel to the fibres is based on the volume fraction of fibres to matrix and is high, compared to a low modulus value at a right angle to fibre direction (Hull and Clyne, 1996).

The majority of composite shafts are manufactured by sheet lamination and use unidirectional pre-preg. plies, with several plies of composite used to produce the shaft. The plies will have various orientations relative to the longitudinal axis of the shaft to give certain mechanical properties. Plies at an orientation of 0^{0} to the longitudinal axis provide bending stiffness, plies at an orientation of 45^{o} to will provide the shaft with torsional stiffness and 90^{o} plies prevent delamination of shaft occurring. The process allows specific mechanical properties for individual shafts to be tailored to the manufacture's demands (Strangwood, 2003; Cheong, 2005).

The stacking sequence of the lamina in the design of the laminate for the specific mechanical requirements must be both "balanced" and "symmetric" in design. This is achieved by off-axis orientation lamina in the laminate are "balanced" by a lamina of negative orientation to the same magnitude (35^{o} , -35^{o}). The "symmetric" design is achieved by the lamina lay up of the laminate being symmetric about the mid-plane of the laminate (0^{0}, 45^{o}, 90^{o}, -90^{o}, -45^{o}, 0^{0}). These design criteria are used in order to balance the residual stresses in the laminate upon curing to retain the shape. However, in certain design aspects having an unbalanced laminate may be beneficial, Figure 1.6, (Hull and Clyne, 1996).

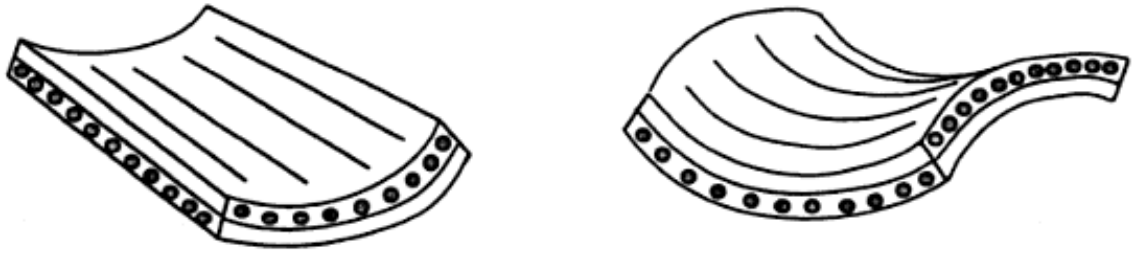

Figure 1.5. Distortion of laminates as a result of non symmetric lay-up (Hull & Clyne, 1996).

Composites behave like viscoelastic materials as a result of the viscoelastic polymer matrix with the continuous fibre reinforcement are embedded in. Viscoelastic materials show creep which is the application of constant stress below that of the material's yield strength resulting in increasing strain with respect to time, once the strain is removed there is a gradual recovery with time. Creep is the result of the polymer chains being stretched in a poly-chain system, the function group of each polymer must rotate for the stretching to occur. As a result the rotation of the function group will not occur until there is adequate space for the rotation and internal forces have been overcome, thus over time with constant stress the strain will increase with respect to time for the polymer (Painter & Coleman, 2009).

Viscoelastic materials are strain rate sensitive, under a high loading rate the rotation of the function group will not occur resulting in the polymer chains to entangle in the poly-chain system, thus the polymer will stiffen due to the entanglement (Painter & Coleman, 2009). The effect of strain rate on IM7/977-2 a carbon/epoxy matrix system was quantified by Gilat, Goldberg & Roberts (2002), the authors tested the composite system under tension at low, intermediate and high strain rates (10^{-5} s^{-1}, 1 s^{-1} and 400 s^{-1} respectively), the composite system showed negligible strain rate sensitivity with respect to modulus between the low and

intermediate conditions, though a reported 250 % modulus increase between the intermediate and high strain rate conditions.

The performance of a shaft is controlled by the dynamic properties of the shaft, though the shafts are characterised by their static properties (simple bending test). Research by Betzler et al (2011) used a range of strain rates (0.01 – 2 s^{-1}) on CFRP panels found that for the strain rates in a dynamic swing (< 0.1 s^{-1}) no significant increase in dynamic stiffness occurs, Figure 1.7. The panels in this research had lay-ups presented in Table 1.3, the panels (C & D) with 0° fibre orientations showed the least strain rate dependency compared to the panel (A) with ± 45° orientation, thus the result of off-axis fibre orientation increases the strain rate dependence of composites.

Table1.3. CFRP panel lay-up (Nils et al, 2011).

Panel	**Lay-up**
A	±45
B	±25 (3), ±45 (16), ± 25(3)
C	0 (1), ±45 (14), 0(1)
D	0-90

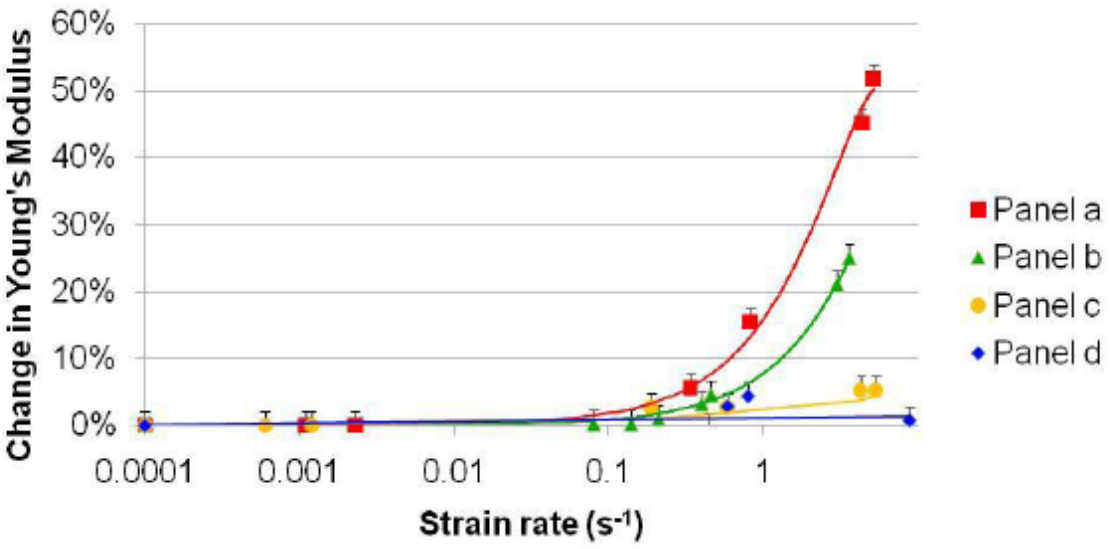

Figure 1.6. The strain rate response of CFRP panels (Betzler, 2011).

1.4.2. Sheet lamination

The production method requires a roll of unidirectional pre-preg of approximately 0.1 – 0.2 mm thickness. The pre-preg is wrapped around a mandrel (gives the inside diameter of the shaft) a set number of times, once achieved the pre-preg is cut (mechanically or by a laser). This process is carried on until the required number of plies and wall thickness (typically 0.6 – 1.2 mm) of the composite shaft is complete, Figure 1.8. The uncured pre-preg shaft will then be cured in a two-piece mould or in a die at 125 – 300 ^{o}C for a period of $1^{1}/_{2}$ – 2 hours depending on the epoxy based resin used in the pre-preg. Once the curing process of the shaft is complete the shaft is then cut to the desired length and polished (Strangwood, 2003; Cheong, 2005). The sheet lamination method is a popular method due to the process being simple and cost-effective.

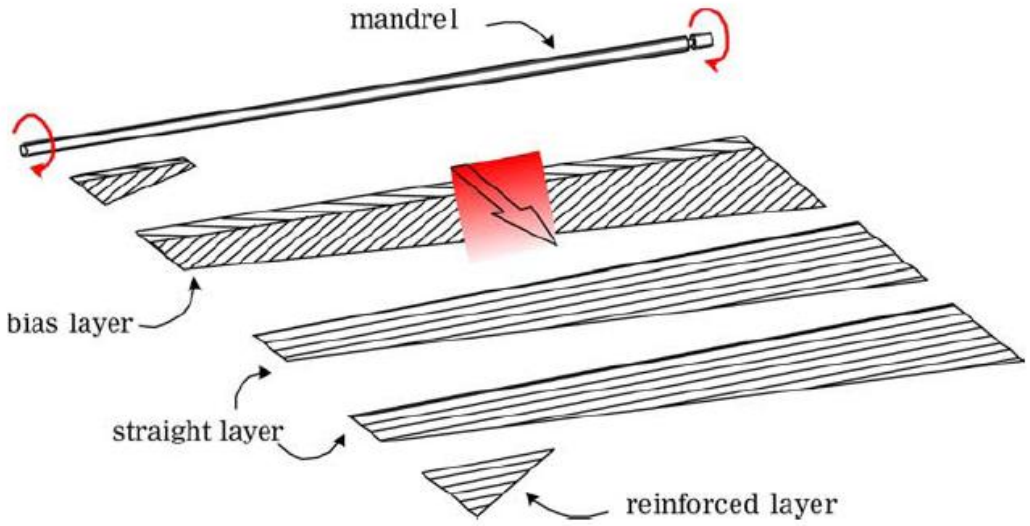

Figure 1.7. The lay-up process of the sheet laminated shaft (Cheong, 2005).

Interestingly, the sheet lamination production method creates inconsistencies in the mechanical performance of the shaft. Research by Werner and Greig (2001) into the inconsistencies in mechanical properties around the circumference of the shaft found a 6 % variation in frequency testing, this research is supported by Huntley (2007) with frequency variations around the circumference of 5.1 %. Further work by Werner and Greig (2001) showed that the 6 % variation in stiffness, when applied to a computational model, could result in a 0.3 m alteration in maximum drive distance.

The inconsistencies around the circumference of the shaft were a result of "seams", the definition of a "seam" is an orientation of the golf shaft that has poorer mechanical properties than the rest of the shaft. The "seams" are a result of a high volume fraction of resin in the area and/or a decreased wall thickness (Huntley, 2007). This is the result of gaps at the end of plies, thus when curing occurs, the outside diameter is defined by the mould and consequently resin seeps into these gaps to produce resin - rich regions. The research by Huntley (2007) showed that the "seams" cause a 34 % variation in Young's modulus around

the circumference of the shaft, though due to geometry constraints of the thickness the specimens did not meet the ASTM D790-92 standards.). Research by Huntley et al. (2006) found that the static stiffness values were similar to the dynamic stiffness values for sheet laminated shafts over a range of strain rates (0.03 – 0.065 s^{-1}) and the presence of seams (orientation of the golf shaft that has poorer mechanical properties than the rest of the shaft) had no influence of the dynamic stiffness values as seen in the static tests

1.4.3. Filament winding

The filament winding method is a manufacturing method that does not produce "seams" as seen in the sheet lamination method. The method requires use of a reel of single or bundled fibre(s) which is known as a filament, the filament is removed from the reel and passed through an uncured resin bath (impregnates the fibre(s)). The filament is then wound around the mandrel and along its length, until the dimensions and properties of the shaft are produced (Matthews, 1994). The shaft is cured in a similar fashion to that of the sheet lamination method by a two-piece mould or forced into a die under the parameters necessary for the epoxy resin to cure, before being cut to length and polished.

Though the filament winding process has no "seam" there are still inconsistencies around the circumference of the shaft, these inconsistencies are a result of resin volume fraction and wall thickness due to the lack of control of resin content for the filament (Matthews, 1994). The filament winding process has the ability to produce a "seamless" shaft and increased flexibility in the design of the lay-up (Howell, 1992), though commercially the process is not utilised to the same degree as sheet lamination due to the slow production process, resulting in greater cost per shaft (Strangwood, 2003). However, the filament wound shafts were strain rate sensitive and showed increased stiffness in the dynamic testing compared to static

testing, the increased dynamic stiffness is a result of higher resin content (greater viscoelastic behaviour) of the shaft due to the manufacturing process (Huntley et al, 2006).

1.5. Summary of Literature Review

The literature review has presented that since the introduction of carbon fibre composite golf shaft in the late 1960's, the shaft's mechanical properties have been analysed by static, quasi-static and dynamic methods with relation to their fabrication process and influence on a golfer's swing. Though the kickpoint position of a shaft has been analysed by static methods, the position of the kickpoint has yet to be characterised by quasi-static and dynamic methods with relation to the fabrication process.

From the literature the kickpoint position along the length of the golf shaft is the result of the stiffness profile (Strangwood, 2003) and ranges between 40 - 60 % in commercial golf shafts (Cheong, 2005; Huntley, 2007). However, this relationship has not been fully quantified with respect to the material properties and dimensions of a golf shaft.

The variation of the mechanical properties around the circumference of the shaft in specific orientations of golf shafts manufactured by sheet lamination was the result of "seams" (Huntley, 2007). The effects of "seams" results in decreased mechanical properties and could influence the stiffness profile in the "seam" orientation, the influence on the stiffness profile could change the position of the kickpoint in this specific orientation.

1.6. Aims & Objectives

The aim of this study is to characterise and quantify the construction method of carbon fibre composite shafts and the subsequent kickpoint position of the shaft. The objectives of this thesis to support the aim are:

- To characterise and quantify the dimensions and material properties of commercially available shafts.
- To characterise the mechanical performance of the commercially available shafts.
- To investigate the influence of the manufacturing method on the mechanical performance of the shafts.
- To investigate the relationship between the dimensional and material properties of the shafts on the subsequent mechanical properties.

2. Method

2.1. Materials & Samples

A range of composite golf shafts from various manufacturers with a range of mechanical properties were used in this study, Table 6.1. The shafts used represent the range of stiffness (ladies, regular and stiff), kickpoints (Low, regular and high) and manufacturing methods (sheet lamination and filament winding) produced by the manufacturers.

Static analysis was performed on all of the shafts for Sections 2.4 - 2.6, this data was analysed to identify the extremes of shaft data in the terms of bending stiffness and kickpoint position. The shafts selected were then analysed by quasi-static and microstructure analysis to characterise the kickpoint position with respect to geometrical and material properties of the shafts.

2.2. Statistical Analysis

In the following sub-sections of the methodology the golf shafts are tested by static, quasi-static and microstructural analysis in their manufacturers flex rated groups (ladies, regular and stiff). An unpaired t-test was utilised to analyse if the geometrical and material properties of the shafts were significant between the manufacturer's flex ratings, if the p value is < 0.05 then the variation between two of the manufacturer's flex rated shafts was stated to be significant. Linear regression was used between dependent and explanatory variable to analyse the variation of the data.

2.3. Dimensional Analysis

All the shafts tested were measured for length, mass, density and taper. The length of each shaft was measured by a ruler to an accuracy of ± 0.5 mm. The mass was measured by digital scales to an accuracy of ± 0.1 g. The diameter of the shaft was measured to investigate taper at 25 mm intervals from the tip by digital callipers to an accuracy of ± 0.01 mm. The density of each shaft was measured by sectioning a small sample from the shaft and placed in an Electronic Densimeter ED-120 T to an accuracy of ± 0.1 gcm^{-3}.

The intra-batch variation analysis for shafts was analysed by Equation 2.1. (Ashby, 1999) and was utilised to derive the subsequent Equations 2.2., 2.3. and 2.4. for the intra-batch variation analysis of length, mass and second moment of area respectively.

Equation 2.1.

$$f = \frac{3.52}{2\pi}\sqrt{\frac{EI}{ml^3}}$$

Where: f is the frequency (Hz)

m is the mass of the shaft (Kg)

l is the cantilever length of the shaft (m)

E is the modulus of the shaft (GPa)

I is the second moment of area of the shaft (m^4)

Equation 2.2.

$$f \propto \sqrt{\frac{1}{L^3}}$$

Equation 2.3.

$$f \propto \sqrt{\frac{1}{m}}$$

Equation 2.4.

$$f \propto \sqrt{\frac{I}{1}}$$

2.4. Bending stiffness Test

The bending stiffness of a shaft was determined by the use of a deflection board, in which the shaft is clamped at the grip end and a load (24.5 N) is placed at the tip end of the shaft, Figure 2.1, the deflection of the tip end of the shaft under a given load is measured and is applied to Equation 2.5.

The bending stiffness of the shafts was analysed at a variable cantilever length (L - 150 mm) and single cantilever length (800 mm) as a result of previous work by Huntley (2007) and Summit (2000) presenting more comparable data for shafts analysed at a single cantilever length.

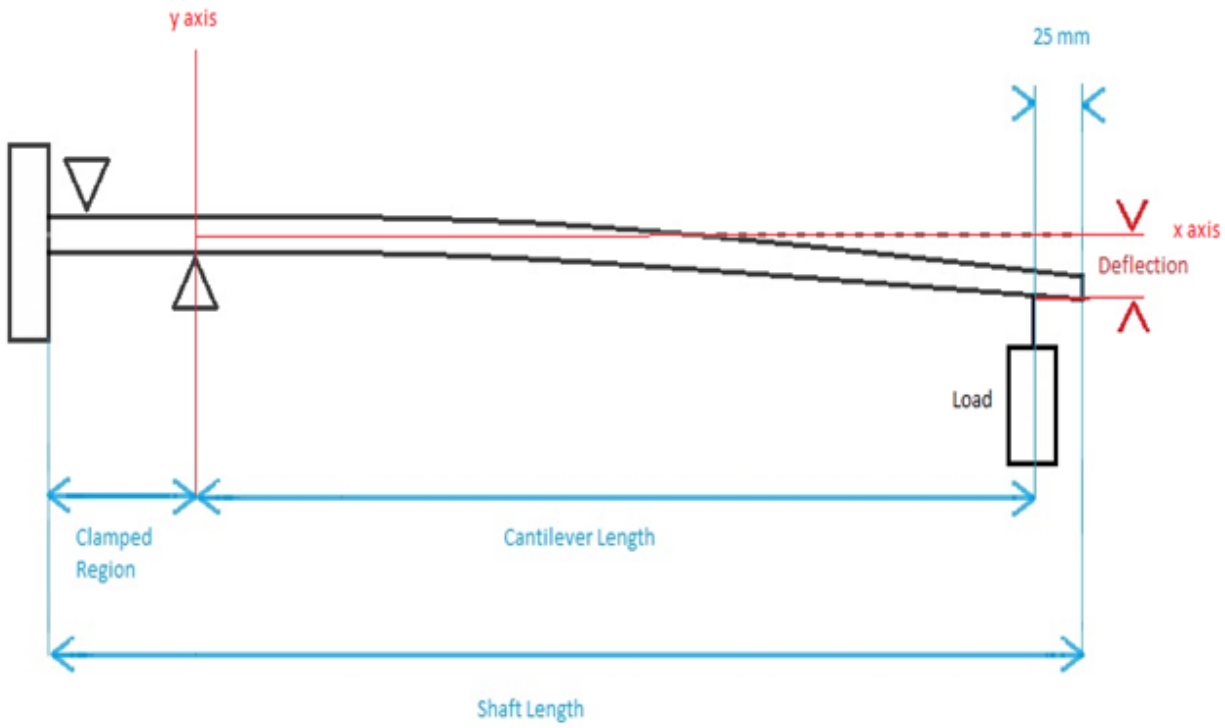

Figure 2.1. Diagram of the deflection board method used for shaft stiffness testing.

Equation 2.5.

$$Stiffness\ \left(\frac{N}{m}\right) = \frac{Load\ (N)}{Deflection\ (m)}$$

2.5. Kick Point Test

The kick point of a shaft is defined as the point at which the separation of a tip-loaded shaft from a straight line from clamped region to tip (measured perpendicularly from that straight line), Figure 2.1, is maximised.

The position of the kick point of a shaft was determined by the use of a deflection board, the shaft was clamped at the grip end and a given load (24.5 N) placed at the tip end of the shaft

to produce deflection. As previously stated in Section 2.4. this analysis was performed at single and variable cantilever lengths for more comparable data.

An image of the tip-loaded shaft was taken and coordinates (x and y) were taken along the length of the deflected shaft from the origin defined as the clamped grip end. A straight line is drawn between the origin and point of max deflection, the angle between the straight line and the x axis is defined as "θ" and obtained by Equation 2.6, Figure 2.1.

Equation 2.6.

$$\theta = tan^{-1}(\frac{y\ max}{x\ max})$$

The x and y coordinates along the length of the shaft are then manipulated by Equation 2.7 to produce x' and y' coordinates, this equation results in the x axis becoming the straight line between grip and tip, Figure 2.2. The x' and y' data is then plotted and the greatest y' value is defines the position of the kickpoint, Figure 2.3.

This is a rigid body rotation so that the x' coordinate will become the radius of the line from the origin to (x, y). For the straight line, x refers to the horizontal axis so that:

Equation 2.7.

$$r = \frac{x}{\cos(\vartheta)}$$

$$x' = \frac{x}{\cos(\vartheta)}$$

y will need to be transformed to y' by a similar amount so that:

$$y' = \frac{y}{\cos(\vartheta)}$$

$$x' = x\cos\theta - y\sin\theta$$

$$y' = y\cos\theta + x\sin\theta$$

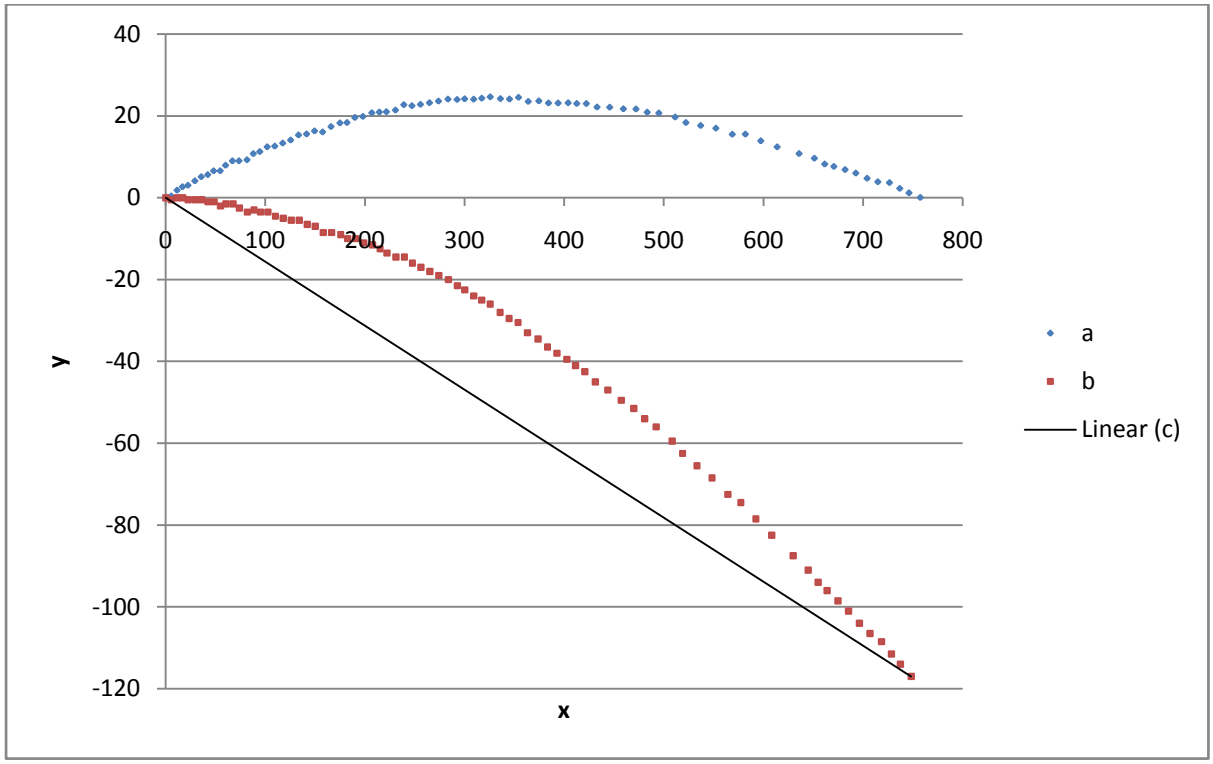

Figure 2.2. a) x' and y' data produced by Equation 2.6, b) original x and y data and c) the straight line between the origin and x and y max.

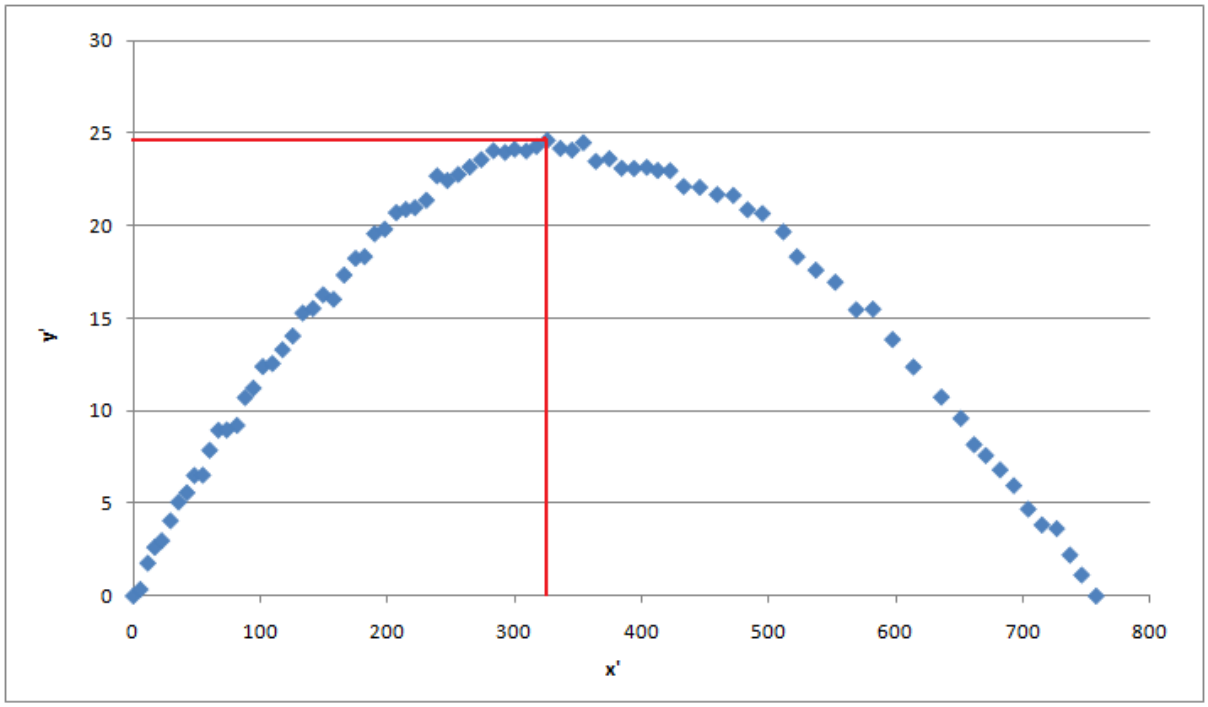

Figure 2.3. The kickpoint data plotted as x' and y', the greatest y' value defines the position of the kickpoint of the shaft.

The kickpoint is generally stated as a percentage of the length of the shaft from the loaded tip to the kickpoint, the distance from the tip of the shaft to the kickpoint was analysed by the distance between each x' and y' coordinate by Equation 2.8.

Equation 2.8.

$$length = \sqrt{\Delta x'^2 + \Delta y'^2}$$

2.6. Assumptions for the Influence of Modulus on Bending Stiffness of Shafts

Assumptions were made utilising Equation 2.9, to produce constant values for second moment of area and length (design variables) to predict the influence of modulus on shaft stiffness.

Equation 2.9.

$$Stiffness = {}^{C\ E\ I}/_{L^3}$$

Where: *C* is a constant for a cantilever test

E is the shaft modulus (GPa)

I is the second moment of area of the shaft (m^4)

L is the cantilever length of the shaft (m)

The data produced from the bending stiffness deflection board test was performed at various cantilever lengths with respect to the shaft length, a single cantilever length was used for the shafts by manipulating Equation 2.9, to produce Equation 2.10 for single cantilever length stiffness.

Equation 2.10.

$$Stiffness_2 = {(Stiffness_1 \; x \; {L_1}^3)}/{{L_2}^3}$$

Where: $Stiffness_1$ is the shaft stiffness (N/m)

$Stiffness_2$ is the shaft stiffness independent of length (N/m)

L_1 is the length of the shaft (m)

L_2 is the normalised length of the shaft (m)

The I value for a shaft was produced by Equation 2.11, using the mean diameter of the tapered shaft for the R_o (Radius Outer), the R_i (Radius inner) value was predicted by using the grip end wall thickness and assuming a constant wall thickness of the shaft. The assumption of a constant wall thickness is supported by previous work by Huntley (2007) presenting constant wall thickness along the length of the shaft, though the wall thickness is greater at the tip ~ 150 mm as a result of tip stiffening.

Equation 2.11.

$$I = {}^{\pi}/_{4}\ ({R_o}^4 - {R_i}^4)$$

Where: I is the second moment of area of the shaft (m^4)

R_o is the radius of the shaft (m)

R_i is the radius outer of the shaft (m)

The Shaft stiffness independent of dimensional variables is calculated by Equation 2.12.

Equation 2.12.

$$Stiffness_3 = {Stiffness_2}\Big/({}^{I_1}/_{I_2})$$

Where: $Stiffness_3$ is the shaft stiffness independent of length and second moment of area (N/m)

$Stiffness_2$ is the shaft stiffness independent of length (N/m)

I_1 is the second moment of area for the shaft (m^4)

I_2 is the normalised second moment of area for the shaft (m^4)

2.7. Bending Stiffness Distribution

The shaft is clamped at 25 mm intervals from the tip to vary the cantilever length of the shaft, the shaft tip has a 2.457 kg mass attached and left for a minute before the subsequent deflection of the shaft is measured by a Solartron B75 displacement transducer and a C55 display console, this process is repeated until the whole shaft length (l_n) is reached, Figure 2.4.

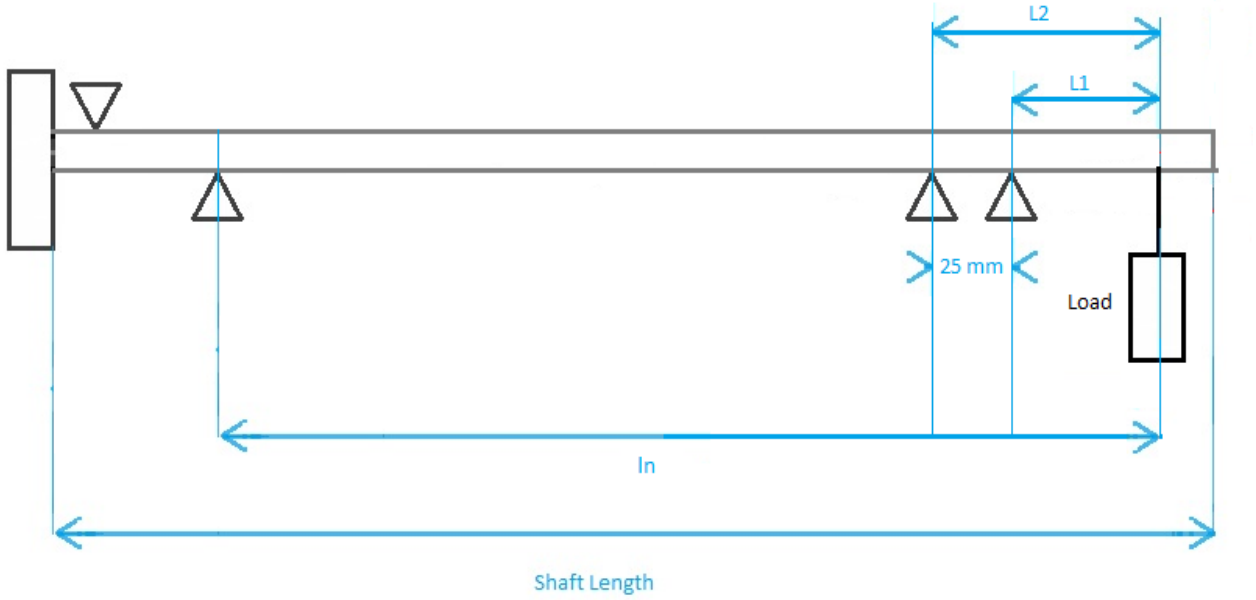

Figure 2.4. Diagram of the method for stiffness profile analysis (adapted from Broulliette, 2002).

A shaft is clamped at a position l_1 and has the stiffness evaluated in the process set above, the shaft is then moved 25 mm and clamped at position l_2 and is repeated until l_n is reached. Equations 2.13 and 2.114 produce the stiffness of the shaft for the relevant cantilever lengths,

though Equation 2.15 can be derived to produce the stiffness of the section $l_{n-1} - l_n$ (Broulliette, 2002).

Equation 2.13.

$$EI_1 = \frac{Fl_1^3}{3w(l_1)}$$

Equation 2.14.

$$EI_1 = \frac{Fl_2^3}{3w(l_2)}$$

Equation 2.15.

$$EI_n = \frac{\frac{1}{3}F[l_n^3 - l_{n-1}^3]}{w(l_n) - \frac{1}{3}\frac{M_{n-1}l_{n-1}^2}{EI_{n-1}}}$$

Where: *EI* is the flexural rigidity of the shaft, comprising of *E* the modulus of the shaft (GPa) and *I* the second moment of area of the shaft (m^4)

M is the bending moment of the shaft (N/m)

w is the deflection of the shaft under the applied force (m)

F is the applied force at the tip of the shaft (N)

L_1 is the initial cantilever length where deflection was measured (m)

L_2 is the new position along the cantilever length to measure deflection (m).

2.8. Frequency Testing

The fundamental bending of a shaft was determined by using a Golfsmith Precision Shaft Frequency Analysis Machine. Figure 2.5. the shaft is clamped at the butt end and has a 205 g (ASTM standard) mass attached to the tip, the shaft is excited by at the tip and the fundamental frequency is recorded in cycles-per-minute (CPM) at an accuracy of ± 1 CPM.

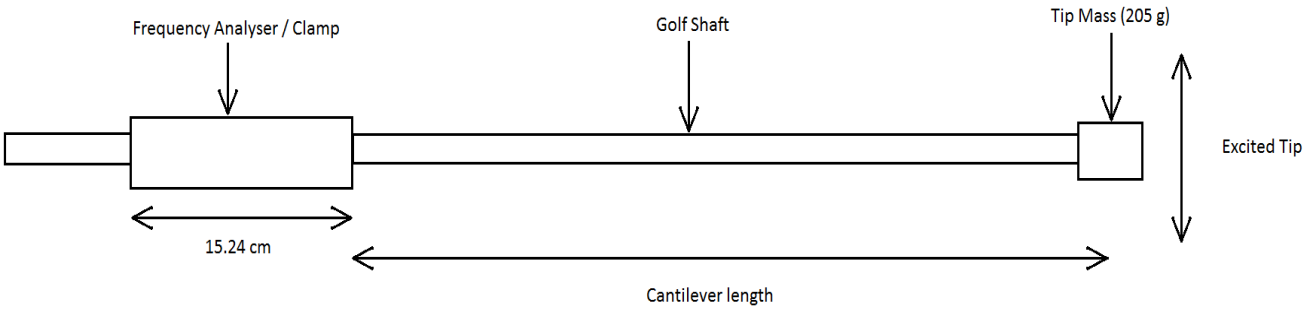

Figure 2.5. Frequency analysis of a shaft excited at the tip.

The frequency distribution around the circumference of the shaft was measured at 10^{o} intervals (anti-clockwise) from 0^{o} to 180^{o} of the shaft circumference. The 0^{o} orientation of the shaft was determined by the placement of the graphics on the shaft as a reference point.

The frequency profile of the shafts with respect to cantilever length was analysed by the shafts clamped at the butt end with the maximum cantilever length (L – 150 mm) at 0^{o} orientation. The frequency was then analysed at various cantilever lengths at progressive steps (25 mm), this method was repeated until the frequency achieved became too high for the Goldsmith Precision Shaft Frequency Analysis Machine to measure (~ 600 CPM).

The relationship between the frequency and stiffness was investigated by combining and rearranging Equation 2.1 and Equation 2.16 to produce Equation 2.17.

Equation 2.16

$$\frac{F}{y_o} = \frac{3}{4}\pi\frac{EI}{l^3}$$

Equation 2.17

$$\frac{F}{y_o} = \frac{6\pi^2}{14.08} f^2 m$$

Where: *F* is the force applied at the shaft tip (N)

y_o is the displacement of the shaft tip (m)

f is the frequency of the shaft (Hz)

m is the mass of the shaft (Kg)

E is the modulus of the shaft (GPa)

I is the second moment of area of the shaft (m^4)

2.9. Static Strain Analysis

Strain analysis for the shafts with the static testing methods was performed by fitting four Kyowa uniaxial strain gauges (type KFG) to the composite shaft, they were placed at the tip (100 mm), butt (700 mm) and either side of the kickpoint position of the shaft (maximum bending curvature) for the assumed location of maximum strain, the strain gauges were

orientated with respect to the longitudinal axis of the shaft. The shafts were tested under the same conditions as Section 2.4. at a single cantilever length, Figure 2.6.

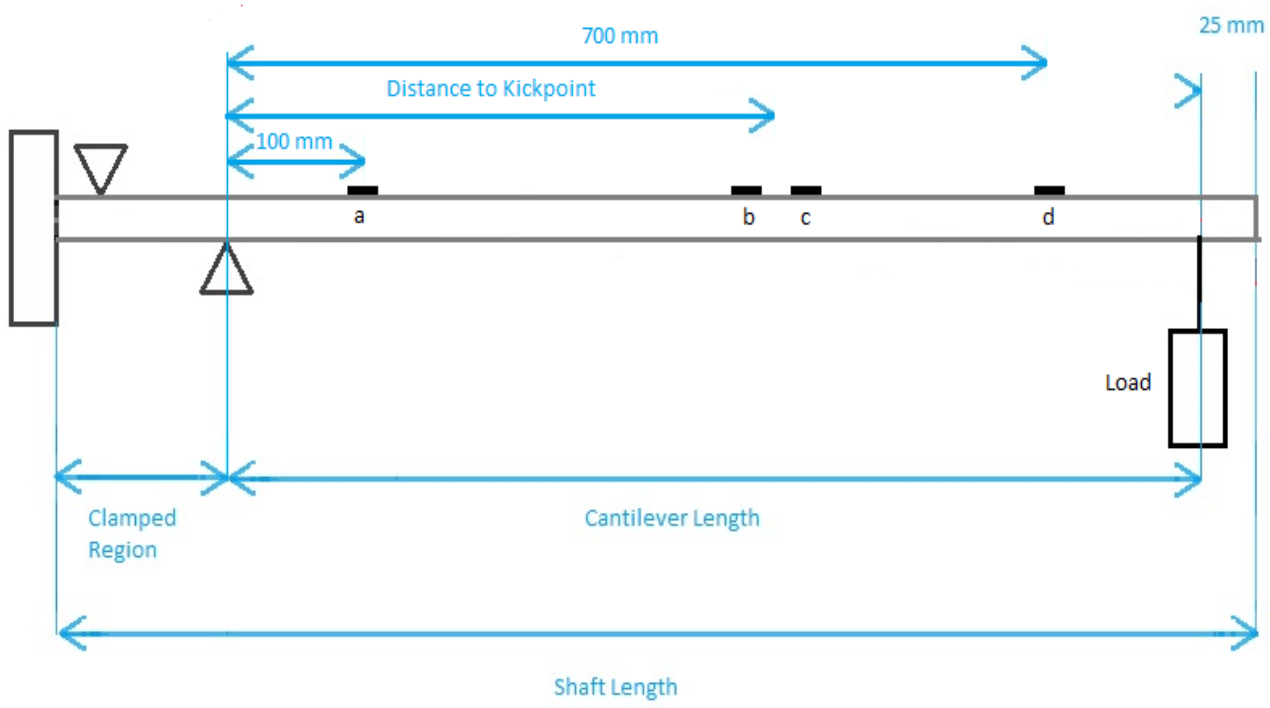

Figure 2.6. Diagram presenting the placement of the strain gauges (indicated by a, b, c and d) along the shaft length.

2.10. Microstructure Analysis

Microstructural analysis was performed on selected shafts along the cantilever length (75, 400 and 800 mm from the tip), at these positions the shafts were sectioned (~ 10 mm sections) and mounted in Bakelite. The sections were ground using the 400, 800 and 1200 grade abrasive paper and then being polished with 6, 3 and 1 µm diamond paste embedded in Struers MDDur, MDDur and MDNap clothes respectively.

The ground and polished samples are then analysed under the Zeiss optical microscope using the KS400 image analysis software. The shafts were analysed for wall thickness, number of

plies, thickness of plies, size of fibres, aspect ratio of fibres (fibre angle) and volume fraction of fibres. The orientation of the fibres "θ" was calculated by using the aspect ratio of the fibres with Equation 2.18.

Equation 2.18.

$$\theta = sin^{-1}\frac{l}{w}$$

Where: θ is the aspect ratio of the fibres (degrees)

l is the length of the fibres (m)

w is the width of the fibres (m)

3. Results & Discussion

3.1 Length

Table 6.2., the length of the shafts range from 896 – 1129 mm, this represents a variable cantilever length range of 746 – 979 mm (the length of the shaft from the tip that acts in the mechanical testing, Section 2.2). Table 3.1, the cantilever length for the shafts was analysed with respect to the manufacturer's flex ratings by T-tests, the cantilever length of the ladies flex shaft with respect to the regular and stiff flex rated shafts was significant ($p = 0.0039$ and 0.048 respectively), though the cantilever length between the regular and stiff flex groups was not significant ($p = 0.51$). The reduced cantilever length of the ladies flex shafts is the result of engineering the shaft length to that of the biomechanics of the female gender's swing (Maltby, 1995).

Table 3.1. The cantilever length ranges for the respective manufacturer flex rating.

Manufacturer's Flex Rating	Cantilever Length Range (mm)	Mean Cantilever Length (mm)
Ladies	746 - 944	892.27 ± 68.5
Regular	822 - 976	944.96 ± 47.78
Stiff	836 - 979	934.09 ± 45.57

The greatest intra batch variation in the batches analysed in shaft length are shown by batch F with a maximum variation of 0.019 m (between 0.972 and 0.991 m), this variation in shaft length could result in a maximum 2.9 % change in shaft frequency with Equation 2.2. Figure 3.1, shows the relationship of percentage change in frequency and percentage change in cantilever length for the shaft batches analysed and strong correlation ($R^2 = 1$) for the relationship.

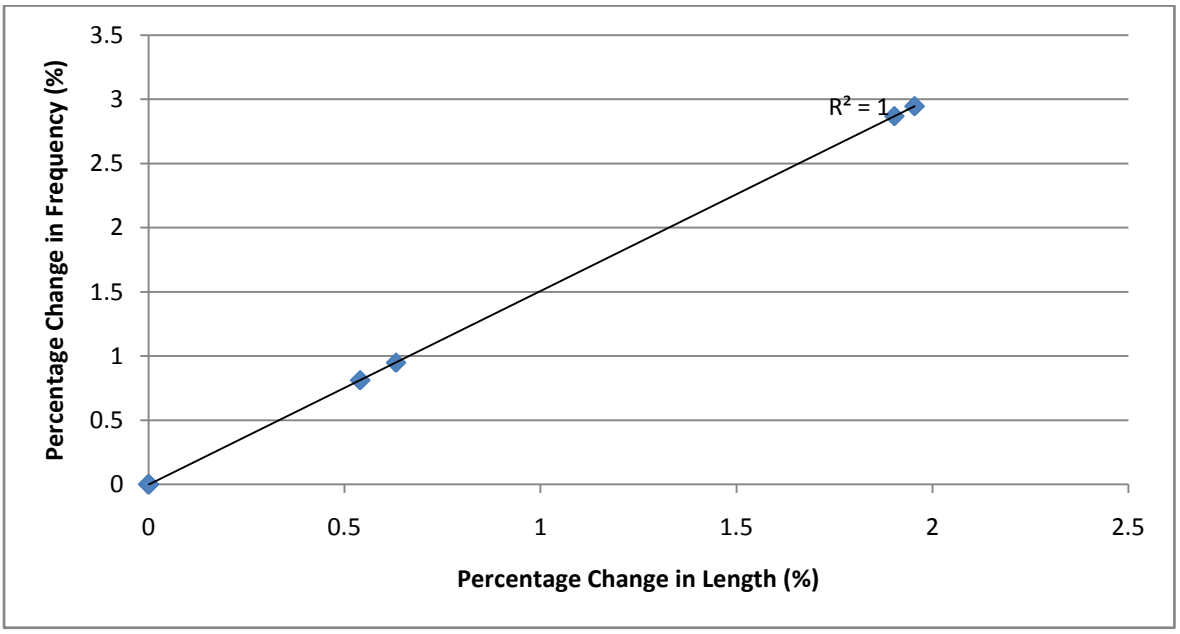

Figure 3.1. The relationship between percentage change in length and percentage change in frequency for batch F.

3.2 Mass

The mass of the shafts analysed in this study range from 107.95 – 48.65 g, Table 6.3, the large range of masses are attributed to variations of the second moment of area, length and density of the shafts. Table 3.2, presents the range and mean masses of the shafts separated into their manufacturer rated flex rating, T-tests between the manufacture flex ratings presented no significance with the respective masses for the flex ratings. This can be

attributed to the density of carbon fibre composites varying between 1.4 and 1.5 g cm^{-3} (Moss, 1971 and Huntley, 2007) and the engineering of the shaft stiffness via second moment of area and modulus.

Table 3.2. Mass ranges for the respective manufacturer flex ratings

Manufacturer's Flex Rating	Mass Range (g)	Mean Mass (g)
Ladies	48.65 - 97.05	63.00 ± 13.42
Regular	55.7 - 107.95	69.76 ± 14.18
Stiff	60.42 - 74.93	67.50 ± 4.72

The shaft batch with the greatest variation in mass is batch K with a mass variation of 11.68 g (between 96.27 and 107.95 g), the variation in mass if all other variables between batch K remain constant could produce a 5.56 % change in shaft frequency with Equation 2.2. Figure 3.2. presents strong positive correlation (R^2 = 0.999) for the relationship of percentage change in frequency and percentage change in mass for the shaft batches analysed.

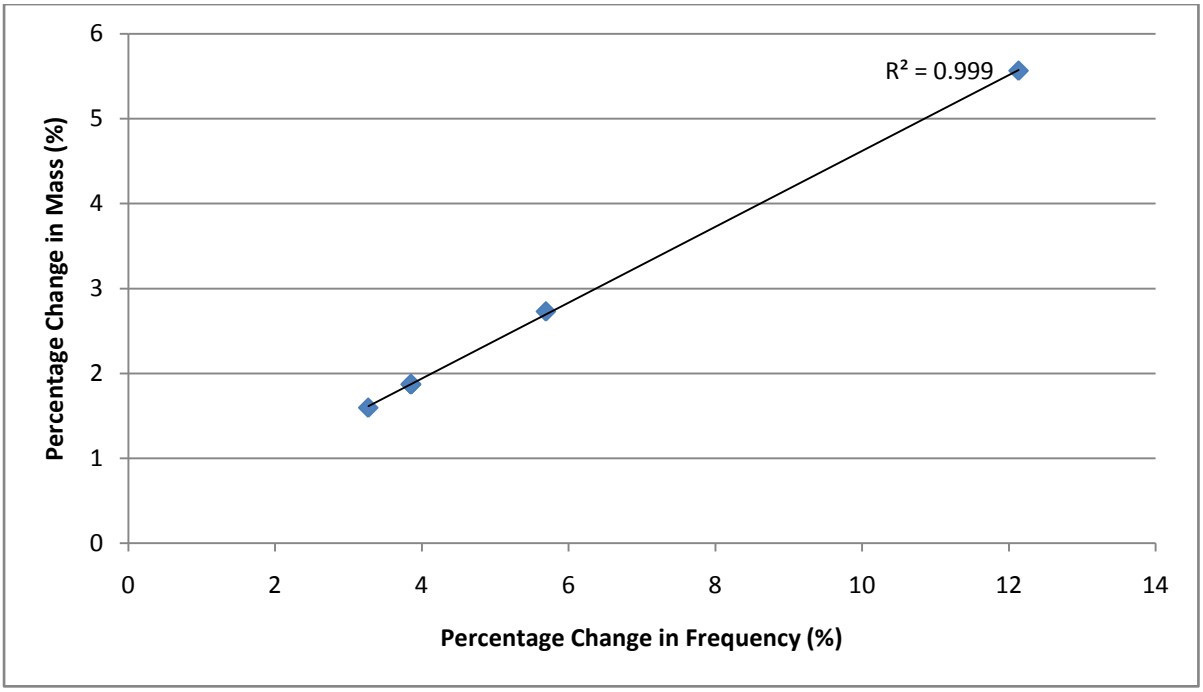

Figure 3.2. The relationship of percentage change in mass and percentage change in frequency.

3.3 Taper

Table 3.3, depicts the taper dimensions for the respective flex ratings to a single cantilever length of 800 mm. The tip diameter for the ladies, regular and stiff manufacturer flex rated shafts is similar due to the typical hosel diameter for a driver head ranging between 8.12 and 8.75 mm (Summit, 2000).The butt diameter for the ladies is less than that of the regular and stiff manufacturer flex rated shafts (13.88 ± 0.75, 14.09 ± 0.62 and 14.51 ± 0.63 mm respectively) and were significant ($p = 0.035$ and 0.042 respectively), though the butt diameter between regular and stiff manufacturer flex rated shafts was not significant ($p = 0.43$). The static shaft stiffness and kickpoint with respect to the taper dimensions will be discussed in greater depth in Section 3.5 and Section 3.8 respectively.

Table 3.3. Taper dimensions for the respective manufacturer flex ratings.

	Manufacturer's Flex Rating								
	Ladies			Regular			Stiff		
	Range	Average	SD	Range	Average	SD	Range	Average	SD
Tip Diameter (mm)	8.03 - 9.51	8.59	0.52	7.73 - 9.4	8.51	0.39	8.33 - 8.72	8.44	0.12
Butt Diameter (mm)	13.01 - 15.19	13.88	0.75	13.04 - 15.11	14.09	0.62	13.5 - 15.43	14.51	0.63

Figure 3.3 shows the taper profiles for a ladies flex shaft (AV), regular flex shaft (BH1) and stiff flex shaft (AS) to a cantilever length of 800 mm. The taper profiles show that the mean tip diameter for the stiff, regular and ladies flex shafts is similar (8.46, 8.42 and 8.41 mm respectively), though the taper for the stiff flex shaft starts earlier in the cantilever length compared to the regular and ladies flex shafts (75, 150 and 150 mm respectively). The taper for the stiff and regular flex shafts finishes prior to the clamped region (675 and 675 mm respectively) and have a greater butt diameter than that of the ladies flex shaft (15.08, 15.06 and 14.49 mm respectively). The earlier onset of the taper in the regular and stiff manufacturer flex rated shafts results in an increase in second moment of area profile for the shafts, thus increasing the stiffness of the shafts by the taper profile influencing Equation 2.9.

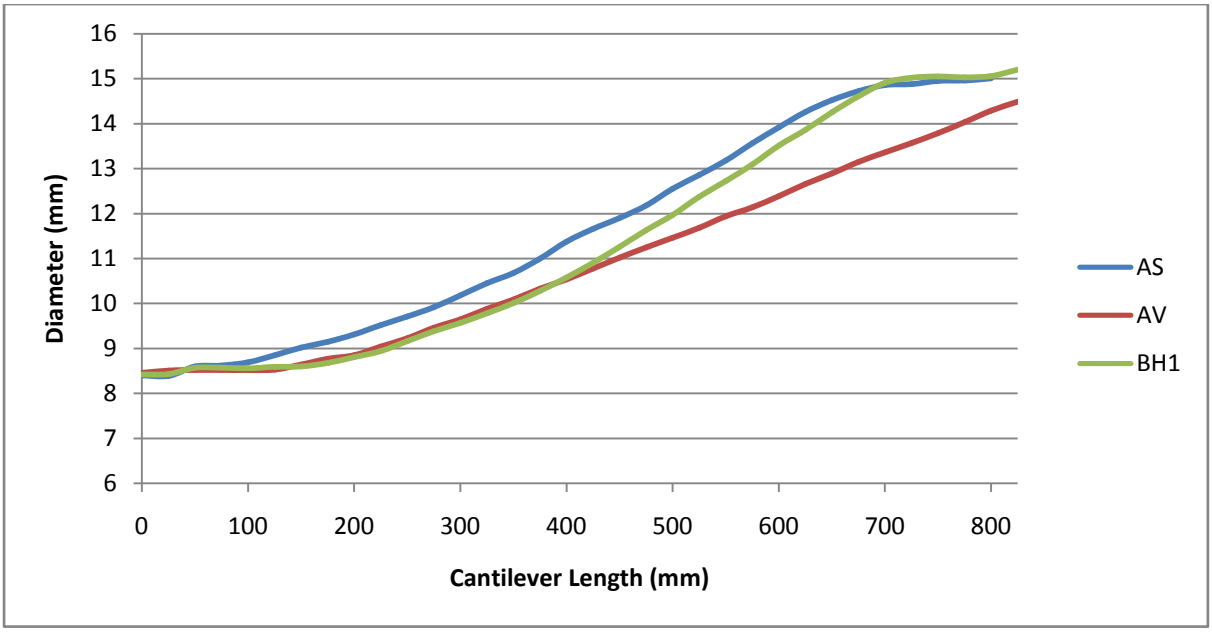

Figure 3.3. The taper profiles for stiff (AS), regular (BH1) and ladies (AV) manufacturer rated flex shafts.

The shaft batch G presented the largest variation in shaft diameter of 3.5 % as shown in Figure 3.4, the taper of shaft G 3 occurs later in the cantilever length and increases at a similar gradient to the remaining shafts in the batch. The influence of the 3.5 % variation of taper can result in a 6.6 % increase in frequency with the utilisation of Equation 2.4.

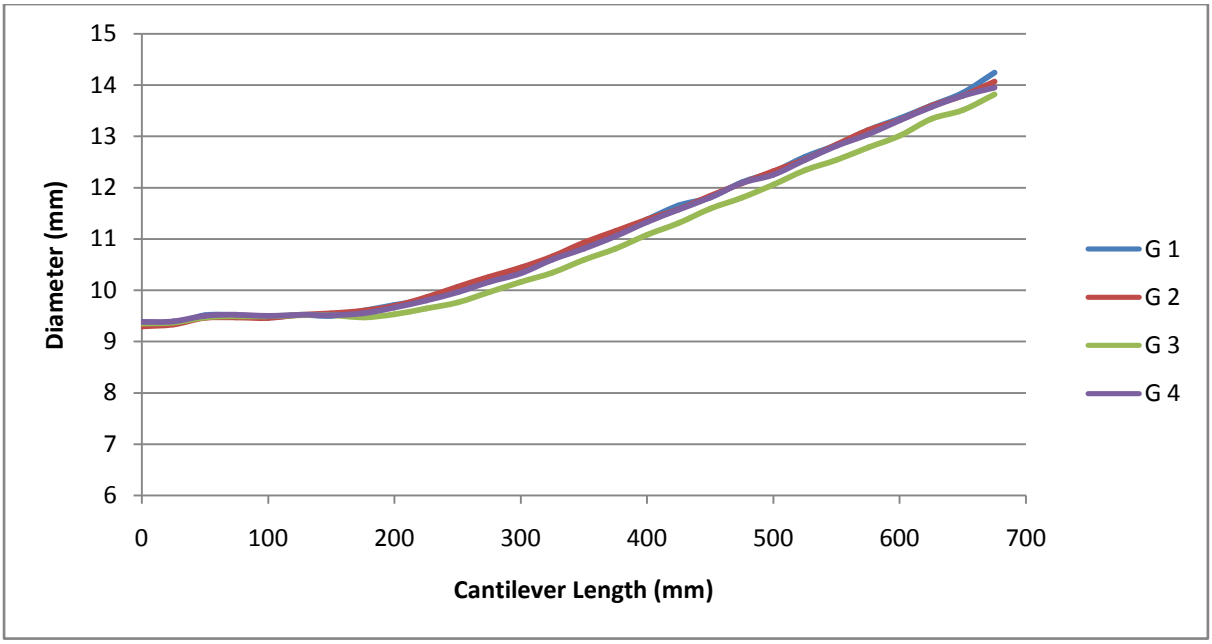

Figure 3.4. The taper profiles for shaft batch G.

3.4 Wall thickness

The wall thickness data is presented in Table 6.4, the mean wall thickness data for the respective manufacturer's flex rated shafts is presented in Table 3.4, the analysis was performed at the butt section of each shaft by digital callipers at ten degree intervals. The mean wall thickness for the ladies manufacturer flex rated shafts is lower than that of the regular and stiff shafts (0.88 ± 0.18, 1.02 ± 0.19 and 0.97 ± 0.12 mm respectively) and was significant for the shafts analysed ($p = 0.019$ and 0.042 respectively), no variation in the mean wall thickness for the regular and stiff shafts was observed ($p = 0.51$).

Table 3.4. Wall thickness data for the respective manufacturer flex rating.

Manufacturer's Flex Rating	Wall Thickness Range (mm)	Mean Wall Thickness (mm)
Ladies	0.56 - 1.23	0.88 ± 0.18
Regular	0.85 - 1.46	1.02 ± 0.19
Stiff	0.70 - 1.09	0.97 ± 0.12

The intra-batch variation in mean wall thickness was greatest for batch K (1.428 – 1.483 mm), the increase in wall thickness and the influence on frequency was analysed via equation 2.4. resulting in a 1.5 % increase in frequency.

The wall thickness variation around the circumference of the shafts was analysed, Shaft BJ is a shaft manufactured by sheet lamination processing and the wall thickness variation around the circumference is shown in Figure 3.5. The wall thickness of the shaft by the sheet lamination method shows a peak at 40 – 100 degrees orientation, the result of the peak in wall thickness can be attributed to manufacturing method by pre-preg and the result of ply overlap (Huntley, 2007), therefore at specific orientations around the circumference the wall thickness can increase due to an increased number of plies in the local area.

The local increase in wall thickness could result in variation of mechanical properties around the circumference of the shaft. By using Equation 2.4. from manipulating Equation 2.1 then the result of local increases in wall thickness can be predicted, by the increase of wall thickness from 0.92 mm to 0.99mm can result in a frequency increase of 0.7 %, this is supported by the Huntley (2007) who showed a 0.9 % increase of frequency with wall thickness variation.

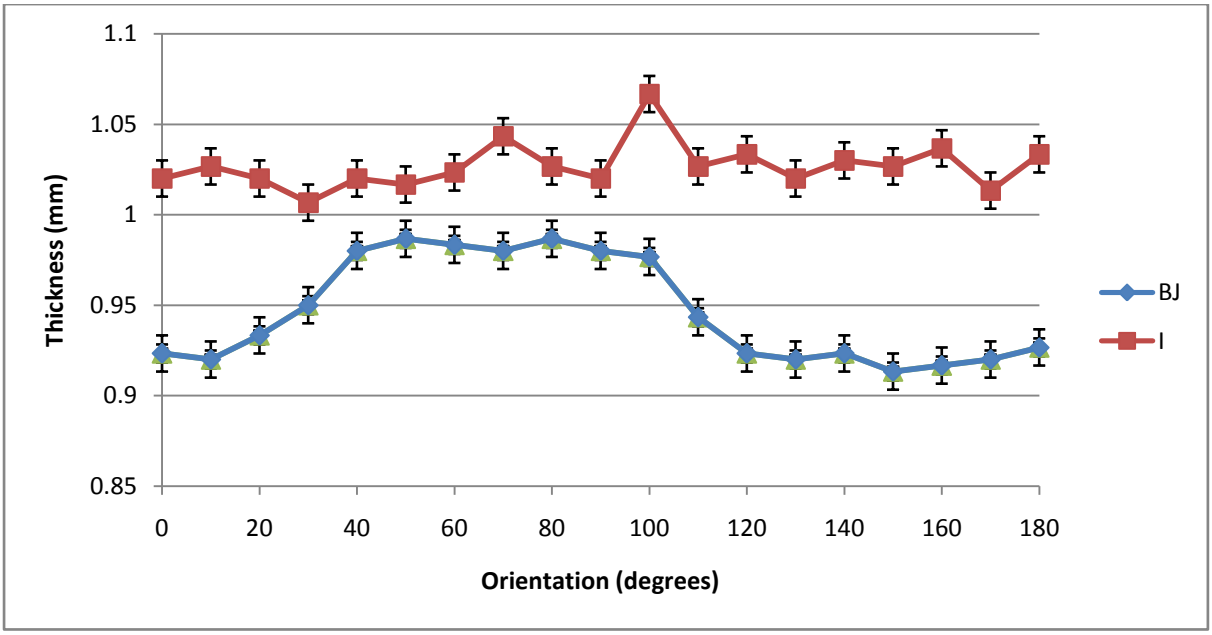

Figure 3.5. Thickness profile of shaft BJ and I with respect to orientation (error ± 0.01 mm).

The filament wound shaft I shown in Figure 3.5 for wall thickness around the circumference of the shaft shows a relatively uniform wall thickness as a result of the manufacturing method and no trend in wall thickness shown as displayed by the sheet laminated shaft BJ. Therefore it can be assumed that the relatively more uniform wall thickness of the filament winding process produces little/no mechanical property variations around the circumference of the shaft.

3.5. Dimensional Analysis Summary

The intra-batch variation of dimensional properties of the composite shafts via length, mass, taper and wall thickness can result in frequency variations of 3.9, 5.6, 6.6 and 0.7 % respectively, this is the result of inconsistencies in the manufacturing process.

The dimensional analysis of the shafts with respect to the manufacturer's flex rating has shown that the flex rating between ladies and regular flex shafts is being engineered by the length, taper and wall thickness (p = 0.0029, 0.035 and 0.019 respectively). However, no significant variation between the regular and stiff flex shafts was observed.

3.6 Stiffness Analysis

Table 3.5. Stiffness ranges for manufacturer flex rated shafts from deflection board testing at variable and single cantilever length.

	Range of Stiffness values (N/m)	
Manufacture's flex Rating	**Shaft Length minus 150 mm**	**Single Cantilever Length (800 mm)**
Ladies	144.2 - 352	242.1 - 498.7
Regular	185.1 - 381.8	367.4 - 508.5
Stiff	198.6 - 309.7	386.3 - 536.3

The bending stiffness of the shafts ranges from 144.2 – 381.8 N/m (Table 6.6.) for shafts tested at variable cantilever length (full length minus 150 mm), Table 3.5, the three stiffness rating from the manufacturers show considerable overlap due to the lack of agreed standards between manufacturers (Horwood, 1995). The stiffness results for the variable cantilever length are not comparable as a result of varying dimensional characteristics of the shafts (length and cross-section variations).

The shafts tested at a single cantilever length (800 mm), Table 3.5, present greater shaft stiffness values for the manufacturer stiffness ratings compared to the variable cantilever length, this result is expected as the decrease in cantilever length of the shaft results in increased stiffness, Equation 2.9. The single cantilever results represent more comparable data, Table 3.5, though the shaft taper alters along the length of the shaft influencing the stiffness values of the shaft, Table 3.6. The overlap of the stiffness ranges for the manufacturer stiffness rating, Table 3.5, is supported by previous work by Summitt (2000) at a single cantilever length of 1.05 m produced deflection value ranges of 0.09 – 0.13 m and 0.11 – 0.15 m for stiff and ladies stiffness manufacturer rated shafts respectively.

The stiffness analysis of the shafts at a single cantilever length in Table 3.6, presents the mean shaft stiffness increasing with the manufacturer's flex rating. Pair wise comparison of the manufacturer's flex ratings showed statically significant results between the ladies to regular and ladies to stiff flex ($p = 0.0059$ and 0.0001 respectively), this result is attributed to the ladies manufacturer flex rated shaft compared to the regular and stiff having decreased wall thickness (0.88 ± 0.18, 1.02 ± 0.19 and 0.97 ± 0.12 mm respectively) and taper (13.88 ± 0.75, 14.09 ± 0.62 and 14.51 ± 0.63 mm respectively).

However, the stiffness values for the regular and stiff (231.3 ± 22.1 and 256.3 ± 20.5 N/m respectively) manufacturer's flex rated shafts also significantly increased ($p = 0.0032$) at a single cantilever length, Table 3.6. Previously in Sections 3.1 – 3.4 no significant dimensional variables between the regular and stiff manufacturer flex rated shafts would result in the increased shaft stiffness, thus modulus of the carbon fibre composites would be influencing the shaft stiffness, Equation 2.9.

Table 3.6. Mean stiffness values of the shafts for their respective manufacturer flex rating.

	Mean Stiffness values (N/m)	
Manufacturer's Flex Rating	**Shaft Length minus 150 mm**	**Single Cantilever Length (800 mm)**
Ladies	173.5 ± 36.6	205.9 ± 31.5
Regular	169.3 ± 22.7	231.3 ± 22.1
Stiff	178.3 ± 18.7	256.3 ± 20.5

The shafts were analysed via their dimensions to investigate the shaft stiffness independent of dimensional variables (Section 2.6), thus from this data the modulus of the shafts can be investigate. The modulus of the shafts analysed ranges from 22.8 -38.2 GPa, the modulus range values for these shafts could be the result of variation in the reinforcement fibres, fibre orientation and the volume fraction of fibres.

The mean modulus values of the shafts increased with the respective manufacturer's flex rating, Table 3.7, the pair wise comparison between the manufacturer's flex ratings confirmed significant increases in mean modulus from ladies - regular and regular - stiff flex manufacturer's ratings ($p = 0.002$ and $.0.0001$). Thus confirming that the flex rating of the shafts by manufacturers is being engineered by modulus, examination of the engineering of composite design for modulus is investigated in Section 3.12.

Table 3.7. Modulus analysis of the shafts from the dimensional data outline in Section 2.4.

Manufacturer's Flex Rating	Modulus Range (GPa)	Mean Modulus (GPa)
Ladies	22.8 – 32.8	28.8 ± 3.14
Regular	26.2 – 35.4	31.7 ± 3.73
Stiff	32.3 – 38.2	35.7 ± 2.52

3.7. Kickpoint Analysis

The accuracy of the testing method for Kickpoint was performed on an aluminium tube of constant modulus and second moment of area (detailed in section 3.10). Research by Strangwood (2003) stipulated that the kickpoint position is dependent on the stiffness profile of the shaft, thus a shaft with a linear stiffness profile would have a kickpoint position of 50 % of the cantilever length. The data from the experiment for the aluminium shaft showed a kickpoint of 49.2 ± 0.64 %, the decreased kickpoint in the experimental to the bending moment being closet to the butt and forcing the kickpoint further down the shaft length (Chou & Roberts, 1994).

The kickpoint data for the shafts is presented in, Table 3.9, Table 6.7 and 6.8, the data shows a range of kickpoints from 46.5 – 53.1 % and 45 – 52.9 % for the single and variable cantilever lengths respectively. The range of kickpoints is within that observed in previous literature 46 – 57 % by Huntley (2007) by utilising the same testing method. The discrepancy

between the 40 – 60 % range observed by Cheong (2005) and results in this thesis can be attributed to the compression test method for kickpoint position determination used by the author, the compression test results in the whole shaft acting (Chou & Roberts, 1994).

The single cantilever lever length shows greater kickpoint values compared to the variable cantilever length, Table 3.9. This is the result of a reduction in length of the cantilever length altering the taper profile (section 3.3) and reducing the second moment of area at the butt section prior to the clamp, thus resulting in a decreased flexural rigidity in the region (Equation 2.9) producing a greater kickpoint vale (Strangwood, 2003). The influence of the flexural rigidity profile of the shaft with respect to kickpoint position shall be quantified in section 3.7.

Table 3.9. Kickpoint position for the shafts at a single (800 mm) and variable (L – 150 mm) cantilever length.

	Mean kickpoint values (%)	
Manufacturer's Flex Rating	**Shaft Length minus 150 mm**	**Single Cantilever Length (800 mm)**
Ladies	50.5 ± 1.7	51.1 ± 1.5
Regular	49.8 ± 2.1	50.2 ± 1.9
Stiff	48.6 ± 2.2	49.4 ± 1.9

3.8. Static Testing Summary

The shaft stiffness data presented significant overlap of the manufacturer flex ratings due to no agreed standards of flex (Horward, 1995), though the data is more comparable when

analysed at a single cantilever length and the mean stiffness values increase with the manufacturer's flex ratings.

The dimensional data between the regular and stiff manufacturer's flex ratings presented no significance in wall thickness and taper ($p = 0.51$ and 0.43 respectively). However, the analysis of the stiffness of the regular and stiff flex shafts presented significance ($p = 0.0032$), thus the manufacturers would be engineering the stiffness via modulus.

The Kickpoint ranged from 46.5 – 53.1 % for the shafts at a single cantilever length, the kickpoint position from previous work by Strangwood (2003) stated that the kickpoint position is a product of the stiffness profile of the shaft and shall be investigated in Section 3.9.

The previous static testing sections were utilised to select the 12 golf shafts represented in Table 3.10. The 12 golf shafts were chosen for further analysis from the dimensions and static testing analysis as they present the extremes of the analysis in terms of kickpoint and bending stiffness at a single cantilever length. These selected golf shafts were analysed by quasi-static and microstructural methods to characterise the kickpoint position with respect to the geometrical and material properties of the shafts.

Table 3.10. Represents mechanical properties of sheet laminated (highlighted blue) and filament wound shafts.

	Single		Variable	
Shaft	**Stiffness (N/m)**	**Kickpoint (%)**	**Stiffness (N/m)**	**Kickpoint (%)**
1C	**262.8**	**52.3**	**196.9**	**51.5**
BJ	**273.5**	**46.8**	**175.5**	**45.9**
AK	**243.4**	**48.7**	**164.9**	**47.5**
AY	**180.8**	**49.1**	**218.0**	**48.3**
AO	**268.9**	**48.1**	**201.1**	**48.4**
D1	**242.5**	**51.2**	**172.6**	**50.7**
AV	**184.2**	**47.3**	**127.8**	**47.8**
BH2	**241.0**	**47.1**	**158.4**	**46.4**
R	**284.5**	**48.1**	**191.1**	**47.6**
I	**262.3**	**52.9**	**195.1**	**52.5**
BE	**210.8**	**53.0**	**161.1**	**52.2**
AF2	**267.0**	**52.0**	**173.7**	**51.2**
BK1	**234.4**	**46.5**	**159.3**	**45.8**
AS	**265.6**	**47.5**	**176.1**	**47.1**

3.9. Frequency Analysis

Frequency analysis is a measurement of shaft stiffness and the relationship between frequency analysis and traditional force/deflection analysis for stiffness will be analysed. The

influence of cantilever length, wall thickness variation and shaft manufacturing route will be analysed with respect to frequency.

Equation 2.17. shows that shaft stiffness (F/y_o) is proportional to the square of frequency. As stated previously Equation 2.1 and Equation 2.16 are designed for tubes with a constant second moment of area and mass per unit length (golf shafts are tapered) and thus will provide inaccuracies, though this will not influence the relationship of stiffness to the square of frequency. The relationship of stiffness being proportional to the square of frequency is shown experimentally by shaft D1 at various cantilever lengths for stiffness and frequency in figure 3.6.

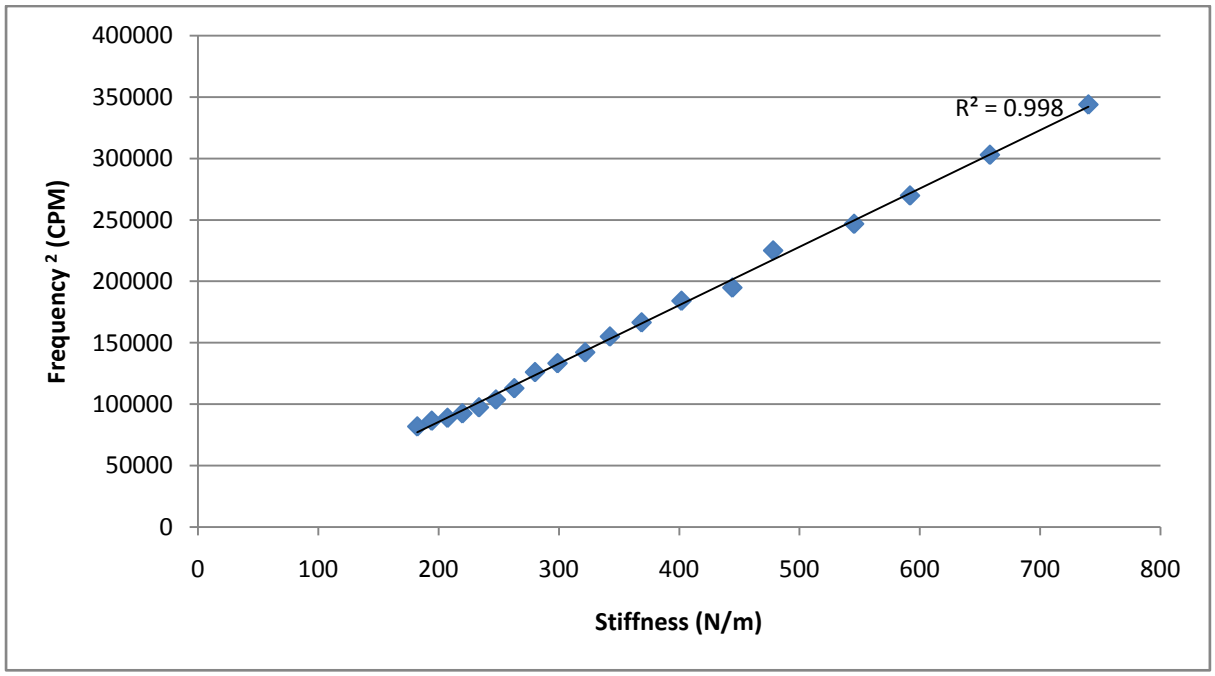

Figure 3.6. Graph showing the relationship between frequency and stiffness for shaft D1.

Figure 3.7. presents the influence of cantilever length with respect to frequency for the shafts D1, BE, I, 1C, AY and BH2. The minimum cantilever length tested to was influenced by the frequency analyser unable to measure at frequencies greater than ~ 600 CPM. The data shows

that frequency is more sensitive to shorter cantilever lengths by a greater gradient in the increase in stiffness, the relationship between frequency and cantilever length is shown by Equation 2.16 and experimentally proven by Figure 3.8.

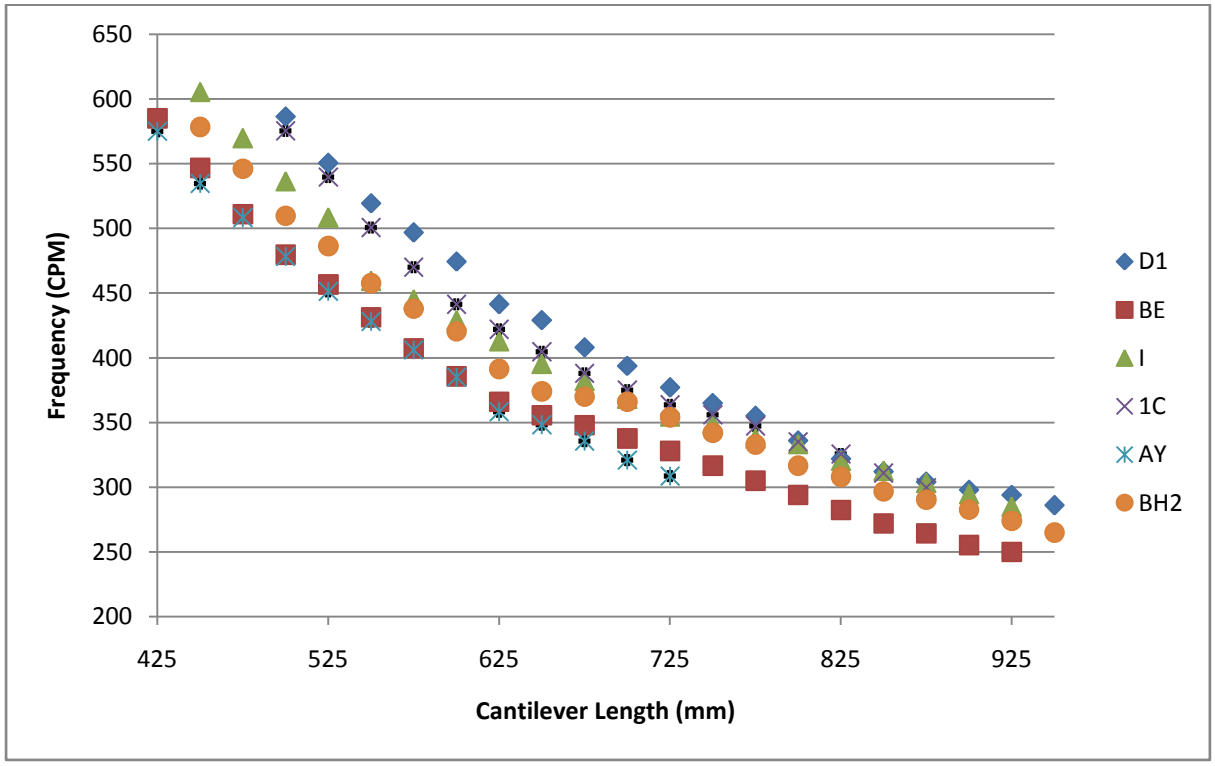

Figure 3.7. Frequency profile with respect to cantilever length.

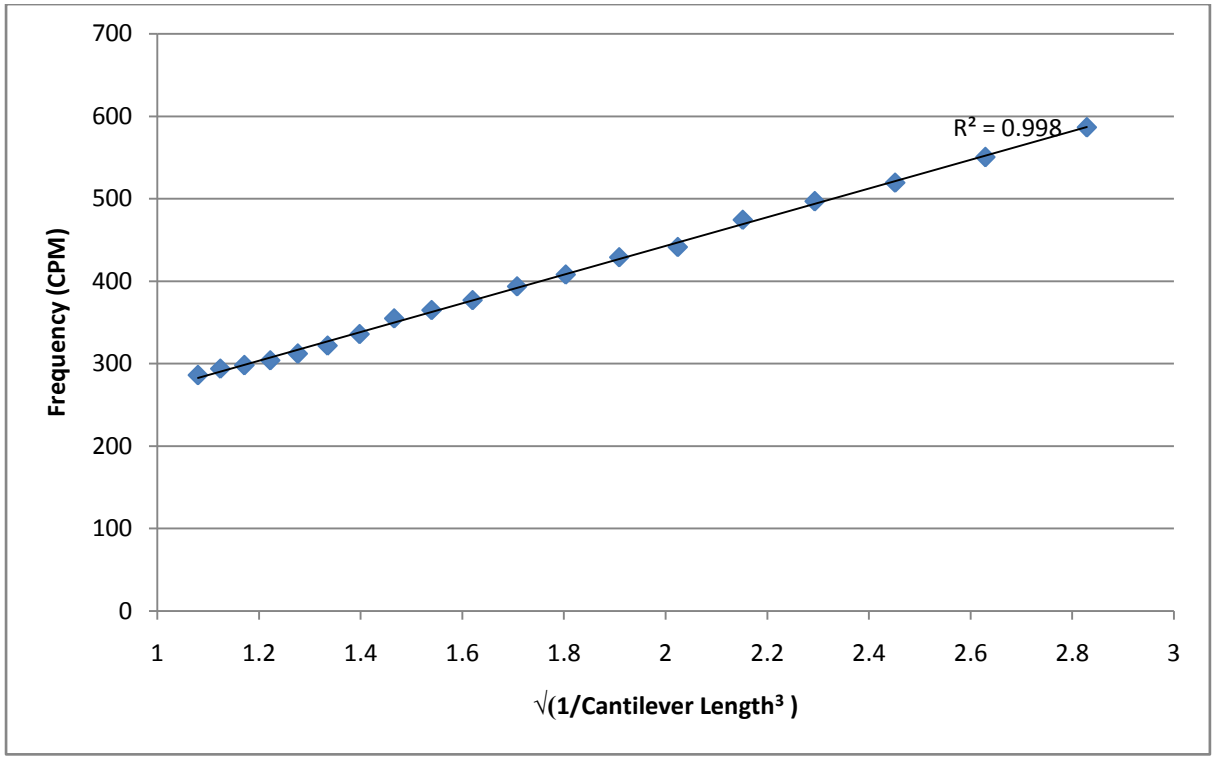

Figure 3.8. The relationship between frequency and √ (1/Cantilever length^3) for shaft D1.

Previously shown in section 3.4 that the thickness varies around the orientation of the shaft and the variation of the thickness is dependent on the manufacturing route of the shaft (sheet lamination and filament wound). The frequency profiles generated will be analysed with respect to wall thickness, manufacturing method and cantilever length.

Table 3.11. shows the mean frequencies at a single (800 mm) and variable (total L – 150 mm) cantilever length, as shown in shaft stiffness testing that the decrease in cantilever length results in greater frequency values as predicted by Equation 2.1. The order of frequency values is the same order shown previously for the shafts tested by static stiffness, Table 3.10. The highlighted data indicates shafts manufactured by sheet lamination compared to that of filament winding, the sheet laminated shafts show greater variation of CPM around their

orientation compared to filament winding (5.33 – 12.00 and 1.67 – 4.00 CPM respectively at the variable cantilever length).

Table 3.11. Frequency data for sheet laminated shafts (highlighted) and filament wound shafts, shaft AY could not be tested at a single cantilever length of 800 mm.

Single Cantilever Length				**Variable Cantilever Length**		
Shaft	**Mean frequency (CPM)**	**Mean range (CPM)**	**Standard deviation of range**	**Mean frequency (CPM)**	**Mean range (CPM)**	**Standard deviation of range**
1C	332.96	9.33	2.80	295.75	7.00	2.37
BJ	331.04	6.67	2.01	267.23	5.33	2.00
AK	304.95	13.67	4.48	267.91	6.00	2.24
AY	-	-	-	300.49	7.33	2.44
AO	329.11	9.67	2.94	289.72	8.67	2.99
D1	337.26	5.33	1.58	283.26	8.00	2.82
AV	260.05	6.33	2.44	240.88	12.00	4.98
BH2	317.74	4.33	1.36	258.96	1.67	0.64
R	327.81	1.33	0.41	284.33	4.00	1.41
I	332.49	2.00	0.60	286.53	2.67	0.93
BE	293.56	3.00	1.02	241.07	2.33	0.97
AF2	328.60	2.33	0.71	273.79	3.33	1.22
BK1	313.67	2.00	0.64	257.96	3.00	1.16
AS	328.32	1.00	0.30	270.95	2.67	0.98

Figure 3.9 presents the frequency profile of shaft BJ that as indicated in Table 3.11. is manufactured by sheet lamination, the frequency profile shows a sine curve nature with respect to orientation with areas of high and low stiffness described as “seams”. The sine curve nature of the frequency profile for sheet laminated shafts is supported by previous literature by Huntley (2007) and Werner & Greig (2001) who presented inconsistencies around the circumference of the shaft with respect to frequency of 5.1 and 6 %.

Figure 3.10, presents the frequency profile of shaft I with respect to orientation, shaft I as indicated in Table 3.11, is manufactured by filament winding. The frequency profile of the shaft shows little variation in frequency (standard deviation of mean range 0.93 at a variable cantilever length) and no “seams” as seen in the sheet laminated shafts, Figure 3.19.

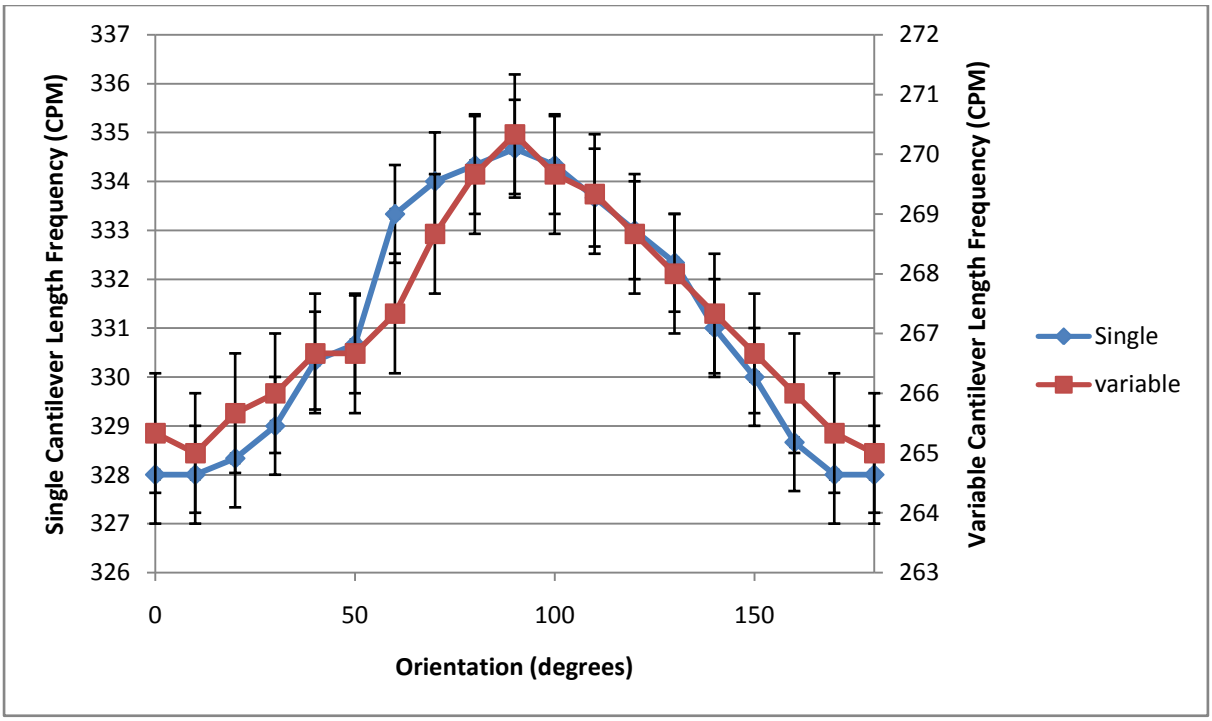

Figure 3.9. Frequency profile of shaft BJ with respect to orientation (error of ± 1 CPM).

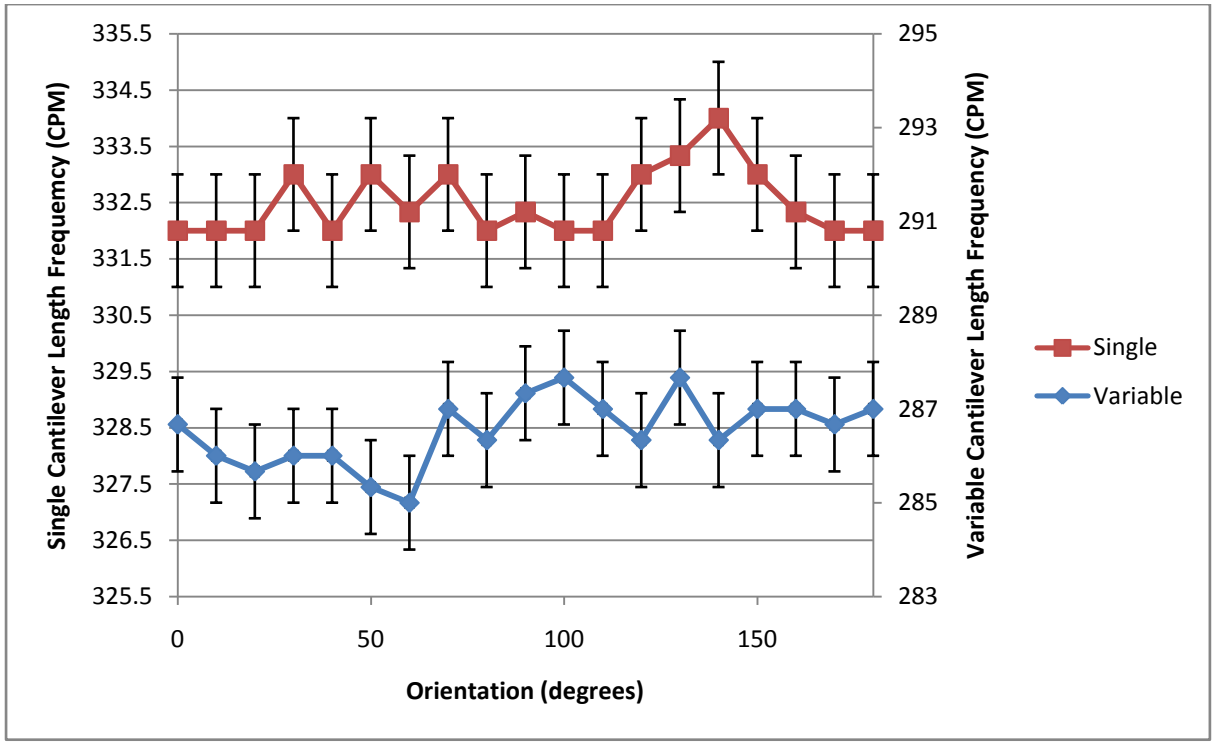

Figure 3.10. Frequency profile of shaft I with respect to orientation (error of ± 1 CPM).

As discussed previously one of the suggestions for the increased variation of frequency in the sheet laminated shafts is a result of the increased wall thickness variation around the shaft circumference compared to that of filament wound shafts (Section 3.4.).

Figure 3.11, depicts the relationship between frequency and wall thickness of shaft BJ (sheet laminated), the localised increased wall thickness of the shaft results in localised increased frequency from the mean frequency between the orientations of 40 and 120 degrees. The wall thickness variation could cause a frequency variation of 0.7 %, though the frequency variation of the shaft is 2.01 % thus microstructural analysis of the shaft is required, Equation 2.1.

Figure 3.15, presents the relationship for wall thickness and frequency of the filament wound shaft I, the manufacturing method filament winding results in little variation of wall thickness

around the circumference of the shaft (1.02 ± 0.013 mm) and this represented by little variation of frequency around the circumference of the shaft (286.5 ± 0.74 CPM).

Section 3.4 stated that the sheet laminated shafts have a single increase and decrease in wall thickness around the circumference of the shaft and show four "seams" (2 high frequency and 2 low frequency), it can be concluded that from the nature of the frequency testing by the oscillation of tension and compression of the shaft at the butt region that the increased thickness at 0 or 180 degrees from the testing position will result in increased frequency.

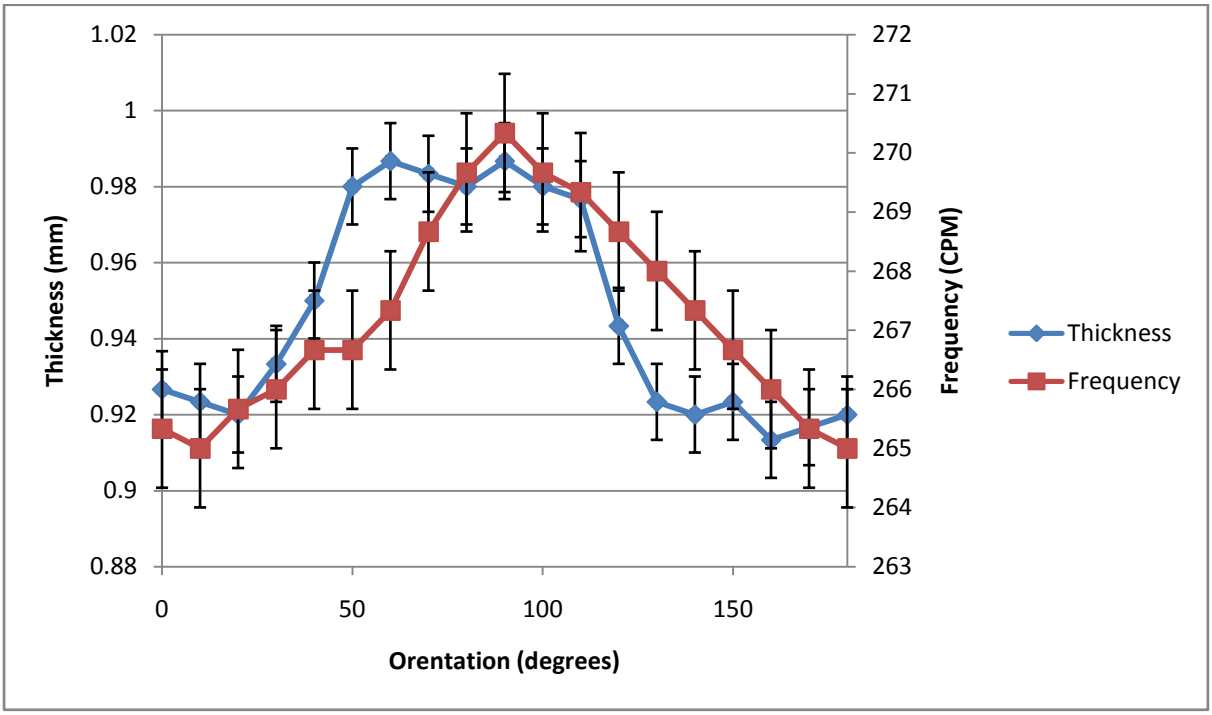

Figure 3.11. Frequency and wall thickness variation for shaft BJ (error of ± 1 CPM).

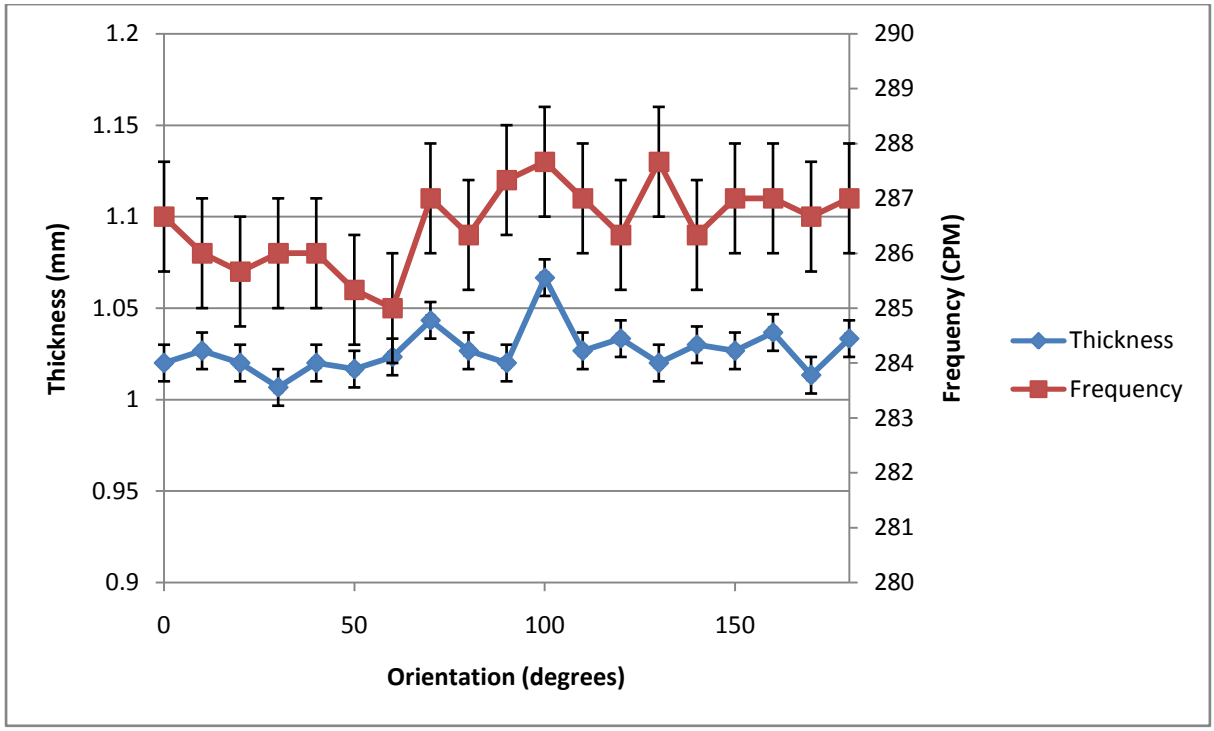

Figure 3.15. Frequency and wall thickness variation for shaft I (error of ± 1 CPM).

The kickpoint position of the sheet laminated shafts, Table 3.11, were analysed at 0^{o} (high stiffness orientation) and 90^{o} to the "seam" position of the individual shafts. The results present no significant variation between the kickpoint position in the high and low "seam" orientations, Table 3.12.

Table 3.12. Table of the kickpoint position of the shafts tested at high and low stiffness "seam" orientations.

Shaft	High	Low
	Kickpoint Position (%)	
1C	52.5 ± 0.42	52.4 ± 0.32
BJ	46.6 ± 0.61	46.9 ± 0.47
AK	48.6 ± 0.45	48.7 ± 0.49
AY	49.3 ± 0.49	49 ± 0.26
AO	48.1 ± 0.33	48.1 ± 0.53
D1	51.6 ± 0.57	51.2 ± 0.51
AV	47.1 ± 0.28	47.3 ± 0.43

3.10. Stiffness Profile

The stiffness profile of the shafts were analysed by the method outlined by Broulliette (2002), the shafts chosen for the stiffness profile analysis represented the upper and lower limits for stiffness and kickpoint from the shafts received, the stiffness profiles will present the method by which the manufacturer engineered the mechanical properties of the shaft.

The accuracy of the stiffness profile test is presented in Table 3.13, the testing was performed on an aluminium tube of a known modulus (74 GPa) and a constant second moment of area (1.26×10^{-10} m^4). The maximum percentage deviation data will be used for the error bars for the stiffness profile analysis.

Table 3.13. Table of the stiffness profile analysis for the Aluminium tube control.

Mathematically Derived EI (Nm^{-2})	Mean EI (Nm^{-2})	SD	Maximum Deviation (%)	RMS Error
9.42	9.58	0.43	10.35	9.50

The stiffness profiles of shaft BJ shows a similar trend to the taper profile of the shaft (Figure 3.13), the gradient of increase of the taper profile corresponds to a subsequent increase in the stiffness profile of the shaft. A similar trend is observed for shaft I that's shows a constant trend in taper increase and as a result is presenting a constant gradient of stiffness profile increase, Figure 3.18.

The shafts BJ and I have similar single cantilever stiffness values (273.5 and 262.3 N/m respectively) however the shaft single cantilever kickpoint positions are 46.8 and 52.9 % respectively. The result of the higher kickpoint position for shaft I is attributed to tip stiffening of the shaft by a constant increase of flexural rigidity, Figure 3.14, while shaft BJ presents a plateau in flexural rigidity until 225 mm, Figure 3.13.

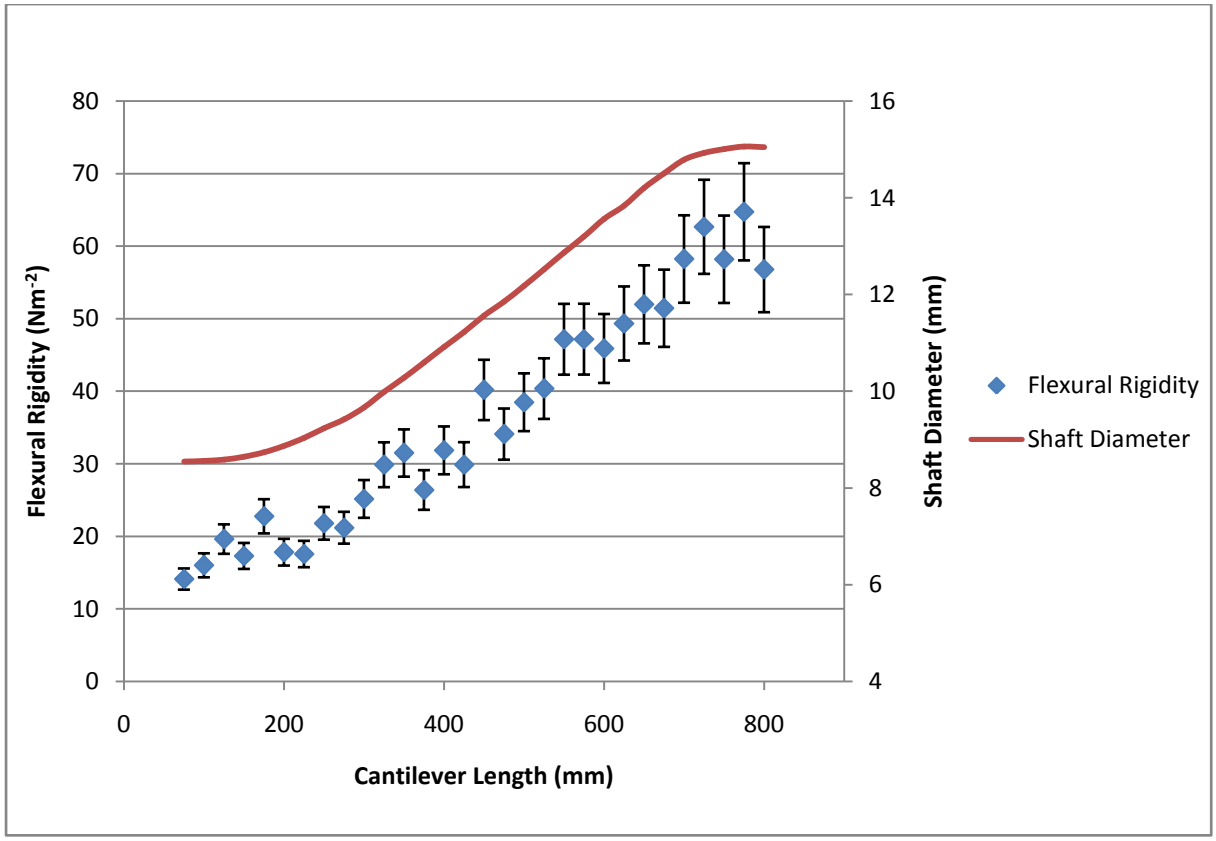

Figure 3.13. Stiffness profile of Shaft BJ with respect to the taper profile (EI error 10.35 %).

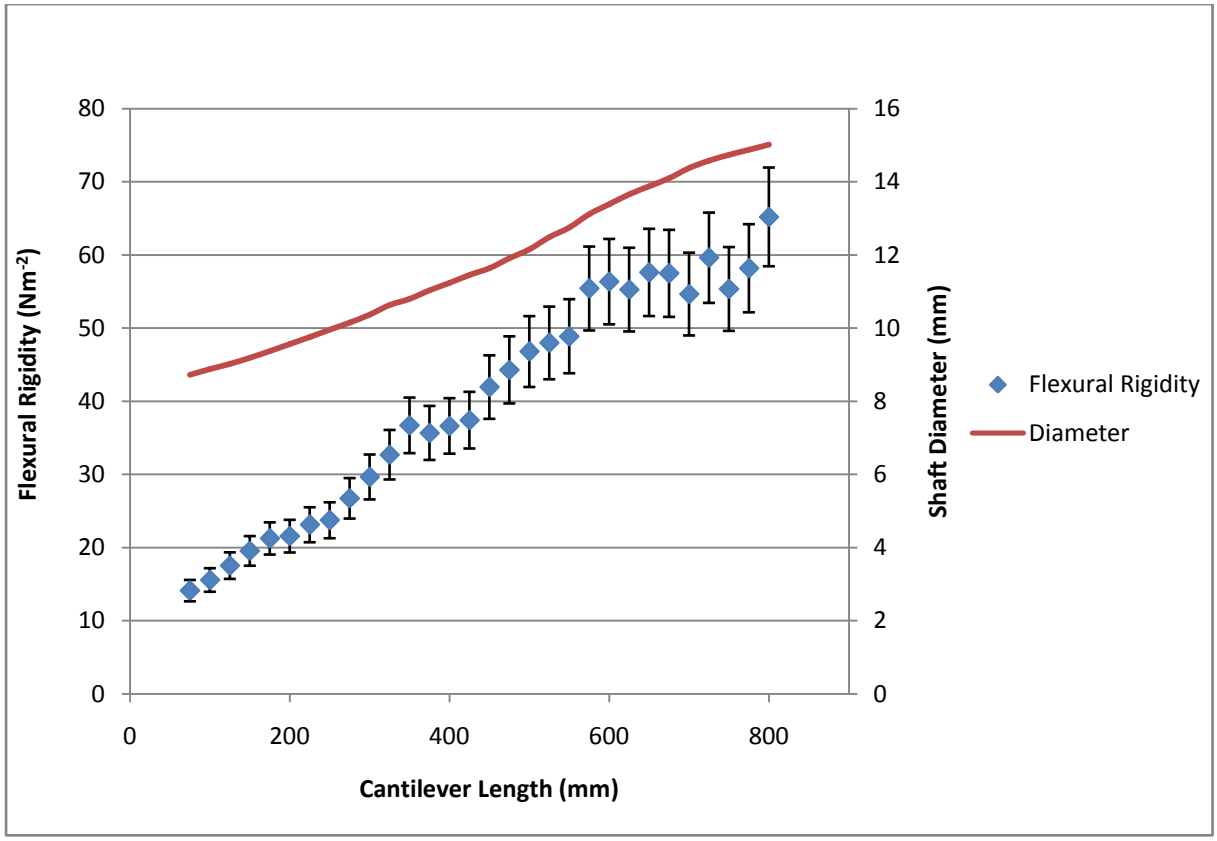

Figure 3.14. Stiffness profile of Shaft I with respect to the taper profile (EI error 10.35 %).

The stiffness profile of the shafts were analysed via linear regression, the analysis provided the gradient of the stiffness profile for each shaft. The gradient of the stiffness profile for each shaft was analysed against the shaft's respective kickpoint position as shown in Figure 3.15, which shows a strong negative correlation of kickpoint point position with respect to stiffness profile gradient (R^2 = 0.77). Although the stiffness profile outline by Brouillette (2002) does not analyse the first 75 mm of the shaft length that will have an influence on the stiffness profile and the subsequent kickpoint position effecting the accuracy of the analysis.

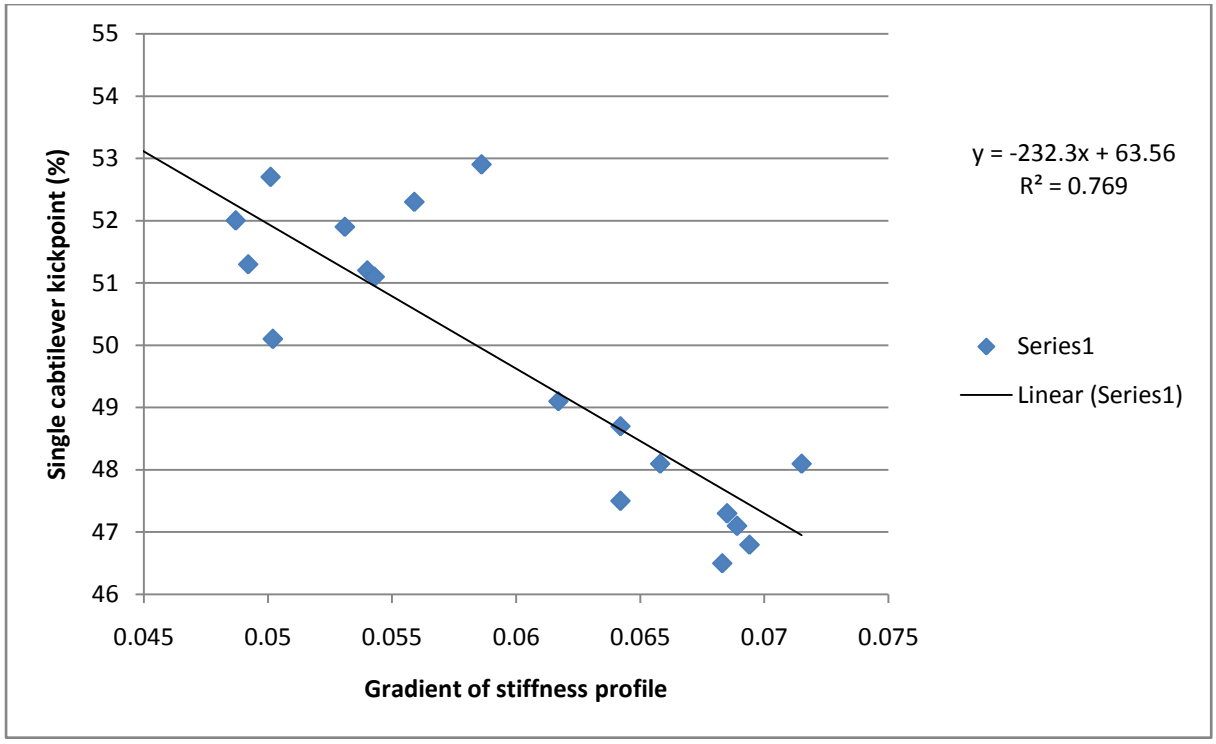

Figure 3.15. The influence of the gradient of the stiffness profile with respect to the kickpoint position.

3.11. Strain Analysis

Shafts AY and BJ were selected for the strain analysis due to displaying the extremes of the data for the bending stiffness analysis at a single cantilever length (180.8 and 273.5 Nm respectively), Table 3.11. The strain analysis presented peak strains of 1710 and 1590 µm/m for shafts AY and BJ respectively, the peak strains observed in the static testing are below that of 6200 µm/m in the dynamic swing of a golf club (Betzler, 2011).

The strain analysis of the shafts with respect to load presents a linear relationship, Figure 3.16, thus the strain ranges experienced in the static testing methods indicate linear elastic stress-strain limits of the composite shafts have not been exceeded.

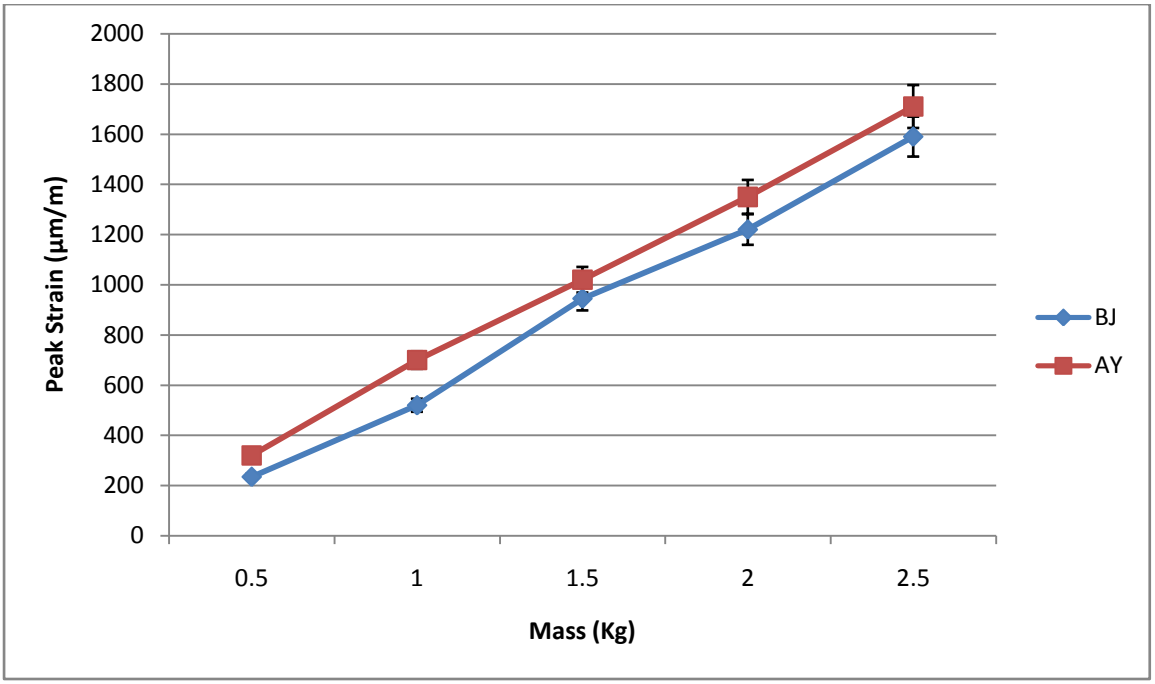

Figure 3.16. The relationship between peak strain and the mass attached at the tip of the shaft.

Differing strain across was observed at the four strain gauges attached along the length of the shaft, the maximum strain observed was for the strain gauges either side of the statically determined kickpoint position (Strain gauges 2 & 3), Figure 3.17. The increased strain in this localised region of the shaft can be attributed to the kickpoint position of the shaft determined by the maximum bending curvature along the length of a shaft, this supports the assumption in previous literature by Betzler (2011) stating that the maximum strain along the shaft's length is located at the kickpoint position.

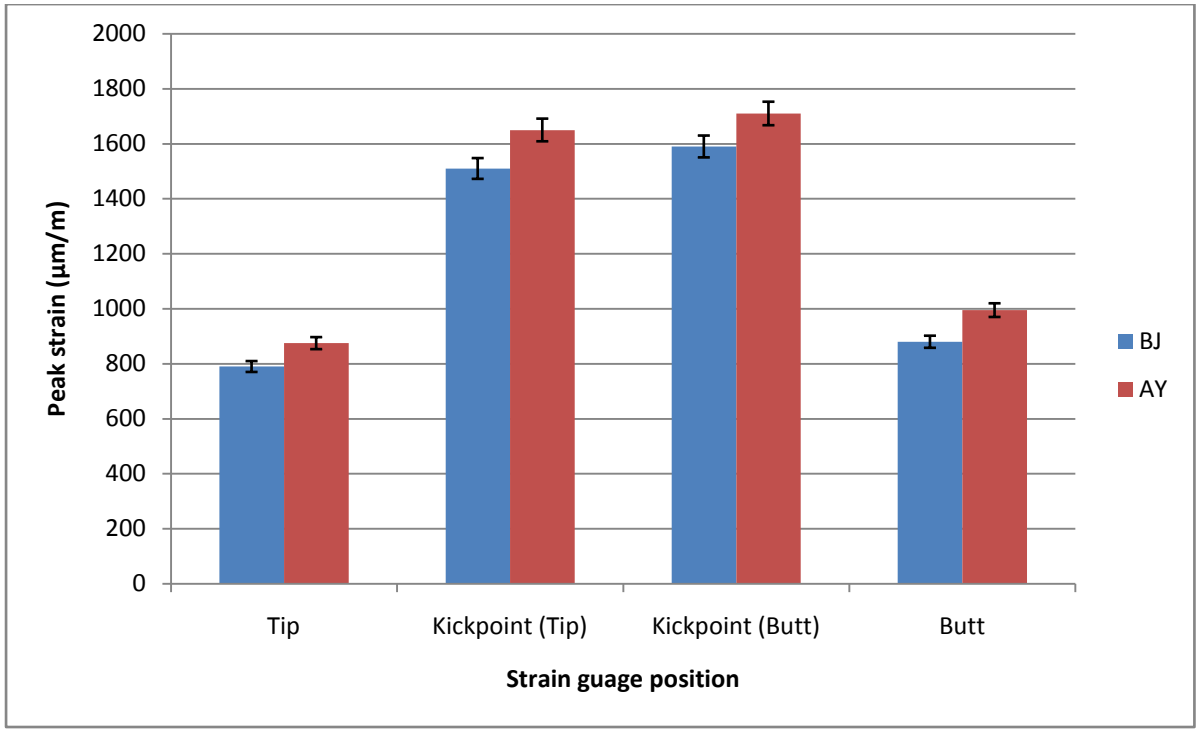

Figure 3.17. Peak strain values for shafts BJ and AY with strain gauge position.

3.12. Microstructure Analysis

The mean ply thickness for the sheet laminated shafts is presented in Table 3.14, the ply thickness ranges from 96.3 – 121.2 µm and is supported by previous work by Huntley (2007) and Slater (2011).

Table 3.14. The ply thickness for shafts with respect to the ply number.

	Ply Number with ply wall thickness (μm) (Ply 10 the outermost ply)									
Shaft	1	2	3	4	5	6	7	8	9	10
BJ	92.1	93.3	94.5	96.2	95.3	95.3	94.2	97.6	103.4	100.6
1C	120.3	121.6	122.5	121.6	123.2	122.9	130.2	132.3		
D1	110.5	111.8	109.2	111.6	112.4	113.3	119.6	122.2		
B	101.5	99.6	97.3	101.2	100.8	97.2	101.4	102.6	112.3	110.6
E2	96.2	97.4	97.8	99.1	98.9	97.5	98.3	96.5	106.48	103.4
AY	119.6	121.1	120.5	117.9	121.3	119.1	124.4	125.8		

The wall thickness profile of the shafts is shown in Figure 3.18, the data presents that all of the shafts have a constant wall thickness to ~ 250 mm along the length of the shaft, at this position the wall thickness of the shaft significantly increases to the tip of the shaft, this process is known as “tip stiffening” of the shaft by adding in a reinforcement layer in the lay-up (Cheong, 2005). The result of tip stiffening on the subsequent microstructure causes significant deformation of the plies and increased resin rich regions with the inclusion of the reinforcement layers, Figure 319.

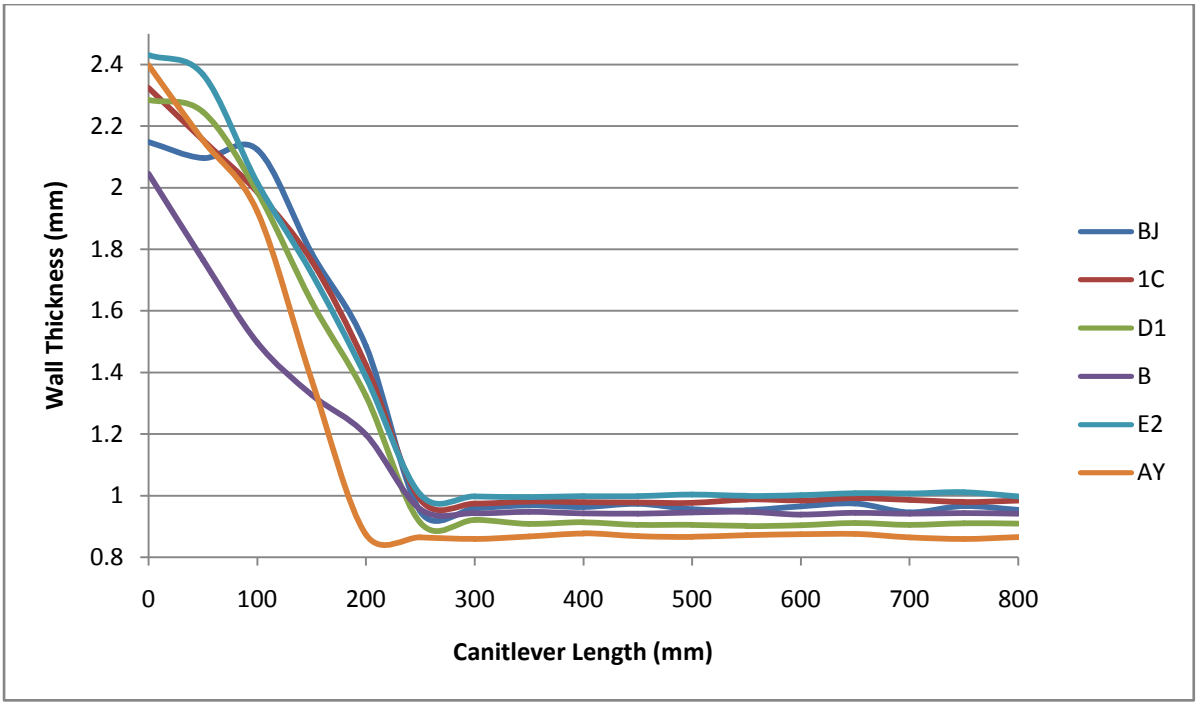

Figure 3.18. Wall thickness profiles of the shafts.

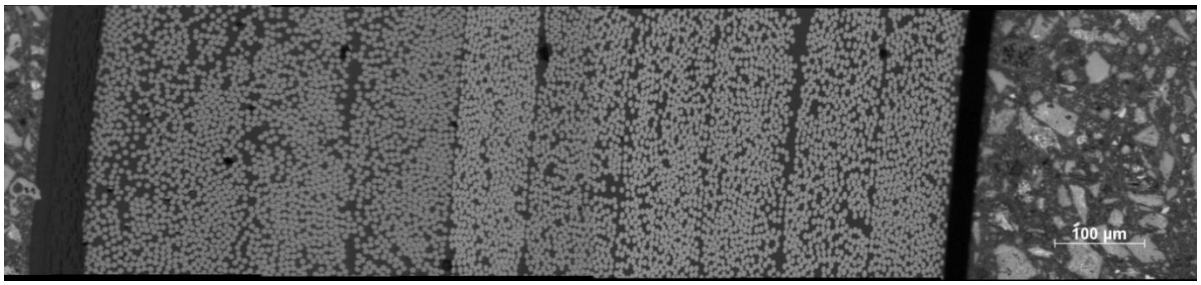

a)

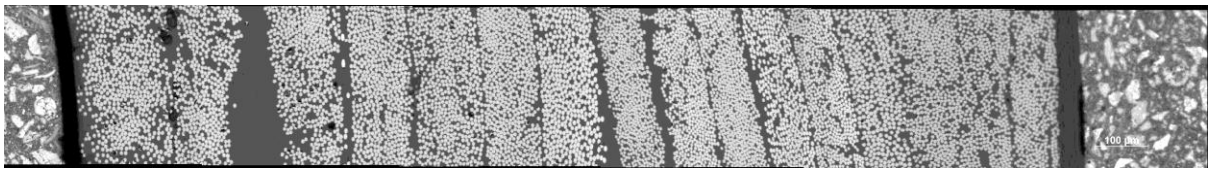

b)

Figure 3.19. Optical micrograph of the thickness profile of shaft E2 at the a) butt and b) tip.

The mean fibre volume fraction of the shafts is shown in Table 3.15, the range of volume fractions for the shafts is supported by previous work by Huntley (2007) and Slater (2011). The volume fractions used by the manufacturers for their respective flex ratings presents no significance.

The data shows the range of volume fractions for the sheet laminated shafts is greater than that of the filament wound shafts (52.7 – 56.7 and 50.6 – 51.4 % respectively), the decreased fibre volume fraction for the filament wound shafts is the result of reduced control of the resin content in manufacturing (Matthews, 1994), the range of fibre diameters for the shafts was 4.7 – 8.2 μm.

Table 3.15. Mean Volume fraction for the shafts.

Shaft	Flex Rating	Manufacturing	Volume Fraction	SD
BJ	stiff	SL	0.57	0.07
1C	Stiff	SL	0.56	0.05
D1	Stiff	SL	0.55	0.05
B	Regular	SL	0.54	0.08
E2	Regular	SL	0.54	0.05
AY	Ladies	SL	0.53	0.06
BE	Ladies	FW	0.51	0.04
I	Ladies	FW	0.50	0.03

Volume fraction for the sheet laminated shafts were analysed with respect to the "seam" location of shafts from the frequency analysis (Section 3.8.). The data showed negligible volume fraction variation at the 0, 45 and 135 degrees orientation, though a significant decrease in frequency was observed for the 90 degree orientation, Table 3.16.

The frequency profile of Shaft BJ plotted with the volume fraction shows the "seam" orientation of the shaft with decreased mechanical properties represented with decreased volume fraction, Figure 3.20. The decreased volume fraction at the "seam" is 8.9 %, research by Huntley (2007) supports this with a volume fraction drop from the overall mean volume fraction by 7.8 %.

Table 3.16. Volume fraction of sheet laminated shafts with respect to frequency (0 degrees is high stiffness orientation).

	Orientation with respect to the frequency profile (degrees)							
	0		45		90		135	
Shaft	Volume Fraction	SD	Volume Fraction	SD	Volume Fraction	SD	Volume Fraction	SD
BJ	0.56	0.07	0.56	0.06	0.51	0.09	0.55	0.07
1C	0.56	0.05	0.57	0.05	0.52	0.1	0.56	0.06
D1	0.55	0.08	0.55	0.05	0.49	0.08	0.54	0.07
B	0.54	0.06	0.55	0.07	0.5	0.06	0.53	0.05
E2	0.54	0.06	0.54	0.05	0.48	0.06	0.54	0.04
AY	0.52	0.08	0.53	0.06	0.47	0.09	0.53	0.06

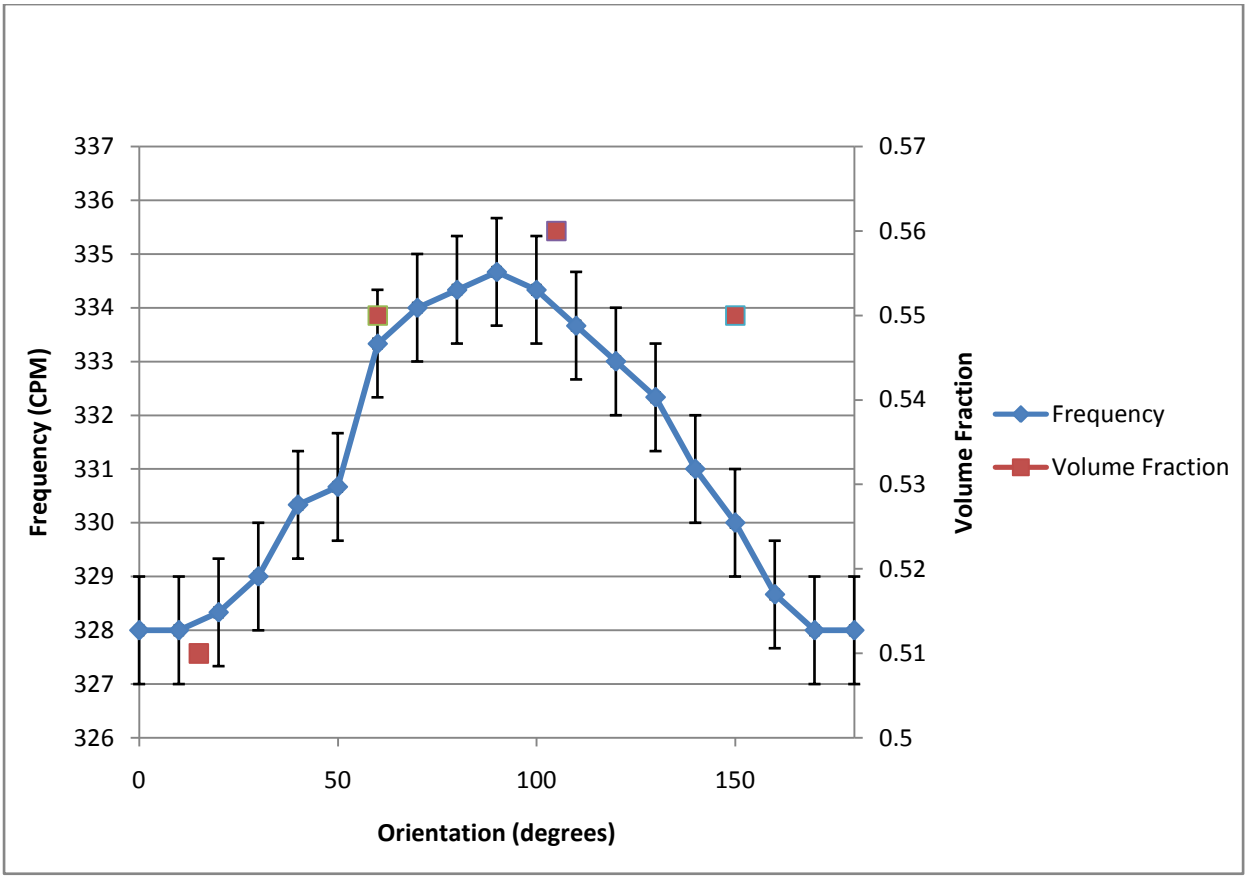

Figure 3.20. Frequency profile of shaft BJ with volume fraction (error of ± 1 CPM).

Table 3.17. Fibre orientation of the sheet laminated shafts.

	Fibre orientation (degrees)									
Sheet Laminated	Ply number (Ply 10 is the outer ply)									
	1	2	3	4	5	6	7	8	9	10
BJ	± 20	± 20	± 20	± 45	± 45	± 45	0	0	0	0
1C	± 30	± 30	± 30	± 45	± 45	0	0	0		
D1	± 45	± 45	± 45	± 45	± 45	0	0	0		
B	± 15	± 15	± 45	± 45	± 45	± 30	± 30	± 30	0	0
E2	± 30	± 30	± 30	± 45	± 45	± 25	± 25	± 25	0	0
AY	± 25	± 25	± 60	± 60	± 45	± 45	0	0		

The fibre orientation of the plies for the shafts analysed is presented in Table 3.17, for the sheet laminated shafts. The fibre orientations for the outermost plies for all of the shafts is orientated at 0^o to carry the tensile and compressive loads experienced on the shaft in the dynamic swing and thus influence the bending stiffness of the shaft.

The stiff manufacturer flex rated shafts present an extra 0^o orientated ply in the outermost layer of the lay-up to increase the bending stiffness of the shaft in the swing plane, previous work by Cheong (2005), Huntley (2007) and Betzler (2011) support this. The innermost plies of the lay-up present off-axis fibres of the shaft, Table 3.15., to carry to the torsional load placed on the shaft to allow the club face to address the ball correctly.

The filament wound shafts BE and I showed fibre orientations of 21.2 ± 2.41 and 14.7 ± 1.98 degrees respectively. The filament wound shafts present no 0 degrees fibre orientation in their microstructure, this is because of the difficulty of engineering 0 degree orientation of fibre in the manufacturing process (Howell, 1992).

The inter-ply resin rich regions of the shafts are displayed in Table 3.18, the inter-ply resin rich regions were identified where the next ply in the lay-up is orientated off axis to the previous ply, Table 3.18. This is observed because during the curing cycle of the pre-preg in sheet lamination the epoxy resin has a low viscosity, this enables fibres of the same orientation to move into the resin rich region, Figure 3.21 a. However, off axis fibres to the previous ply have their movement restricted and are unable to move into the resin rich regions resulting in a greater inter-ply resin rich region, Figure 3.21 b, research by Slater (2011) presented similar findings with regards to the size of “seams” in sheet lamination manufacture of shafts.

Table 3.18. Inter-ply resin rich regions.

	Resin rich region between plies (μm)								
Sheet Laminated	ply 1 - 2	ply 2-3	ply 3-4	ply 4 - 5	ply 5 - 6	ply 6 -7	ply 7 -8	ply 8 -9	ply 9 - 10
BJ	2	3	12	4	3	14	0	0	0
1C	7	6	15	5	12	0	0		
D1	3	14	5	2	8	0	0		
B	6	15	3	4	17	2	3	9	0
E2	2	4	11	4	12	1	4	7	0
AY	2	14	0	8	3	11	0		

Figure 3.21. Optical micrograph of a) the inter-ply resin rich region between two plies of the same orientation and b) plies that are orientation off-axis to the previous ply.

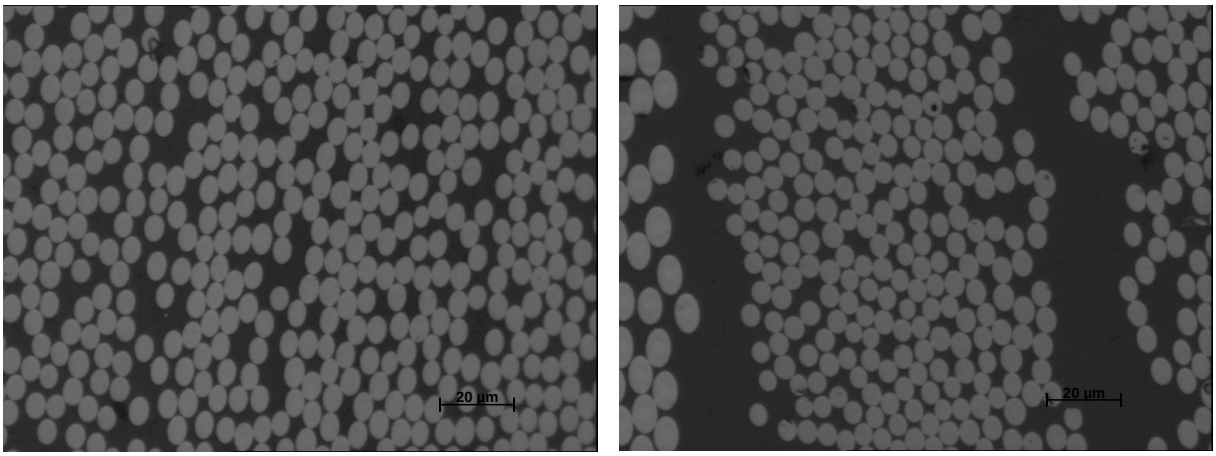

The sheet lamination manufacturing process produces “seams”, as showed previously the “seams” result in reduced mechanical performance of the shaft in specific orientations in a quasi-static test (Section 3.9) as a result of a reduced volume fraction, Table 3.16, and wall thickness, Figure 3.5.

The “seams” in sheet laminated shafts is due to manufacturers using various off axis fibre orientations to engineer the mechanical properties of the shafts in the lay-up process, this produces a void as a result of ply-overlap as shown in Figure 3.22. The fibres are constrained due to their off axis orientation and cannot move into the in the curing cycle, the large resin rich region causes the reduced mechanical properties.

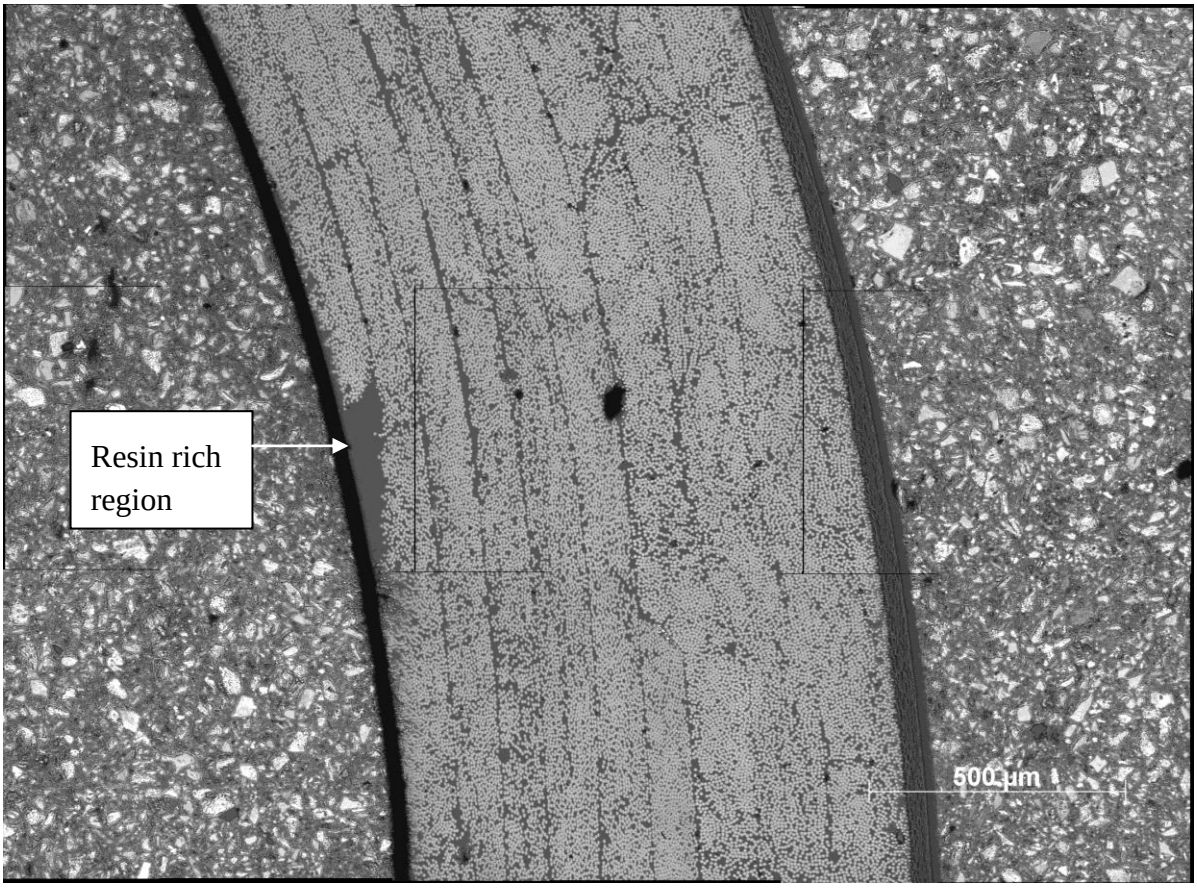

Figure 3.22. Optical micrograph of shaft BJ (800 mm) of the resin rich region as a result of ply over-lap.

4. Conclusions

- The dimensional intra-batch variation of the shaft during manufacture on the length, mass, taper and wall thickness can result in a 2.9, 5.56, 6.6 and 0.7 % increase in the frequency of the shaft respectively.
- The dimensional analysis of the shafts with respect to the manufacturer's flex rating presented significant engineering of the length, taper and wall thickness ($p = 0.0039$, 0.035 and 0.019 respectively) between the ladies and regular flex. Though, no significance was analysed between the dimension of the regular and stiff flex shafts.
- The stiffness of the shafts ranged from 144.2 – 381.8 N/m and 242.1 – 536.3 N/m at a single and variable cantilever length respectively, the manufacture's flex rated shafts present significant mean stiffness values between the ladies – regular and regular - stiff flex rated shafts ($p = 0.0059$ and 0.0032 respectively).
- Kickpoints range from 46.5 – 53.1 % and 45 – 52.9 % for the single and variable cantilever lengths respectively, the position of the greatest strain (1710 μm) along the shaft length is located at the kickpoint position of the shaft in a static bending test.
- The frequency variation around the circumference of the shaft was greatest for shafts manufactured by sheet lamination compared to those of filament winding (4.8 % and 0.2 % respectively), the variation of the frequency around the circumference of the sheet laminated shafts could result in a frequency variation of 0.7 %.
- Kickpoint analysis of the shafts at low stiffness orientations (0^0 to the "seam" orientation) and high stiffness orientation (90^0 to the "seam" orientation) presented no measurable change.

- Stiffness profile on kickpoint of the shaft analysed via linear regression presented a strong negative correlation with the kickpoint position along the shaft's length (R^2 = 0.77).
- The size of the inter-ply resin rich regions are dependent on the fibre orientation in the lay-up process, fibre orientations off-axis to the previous ply showed measurable resin rich regions as a result constrained fibres in the curing process.
- The "seams" caused in the manufacture process result in significant mechanical property variation around the shaft due to a reduction of the fibre volume fraction compared to that of the mean volume fraction by 8.9 %.

5. Further Work

Whilst this study has characterised the influence of parameters such as wall thickness, diameter and modulus on the stiffness profile and the subsequent kickpoint position in commercial shafts, the study has also identified a number of key areas for further research in the identification and behaviour of the kickpoint in the composite golf shaft.

The commercial shafts in this study were examined via static and quasi-static analysis, yet the golf swing is dynamic. Thus strain rate analysis of the commercial shafts over the strain rates experienced in the dynamic swing of 0.09 s^{-1} (Betzler, 2009), though strain rate analysis has been performed on the influence of strain rate on stiffness (Huntley, 207) it has yet been confirmed the influence on the kickpoint position of the shaft.

Finite Element Modelling (FEM) of shafts with various taper designs and ply lay-up to analyse the stiffness profile of the shaft and subsequent kickpoint position, using strain rate analysis of the composite shafts the dynamic mechanical performance of the shaft can predicted.

This study has shown that the kickpoint position is the result of the gradient of the stiffness profile. Using this knowledge a range of composite shafts can be manufactured to produce the extreme kickpoint positions for composite shafts viable for the commercial market. The manufactured shafts could then be tested to investigate the influence of kickpoint position on dynamic loft, club head speed and drive distance.

6. Appendix

Table 6.1. List of Materials.

Manufacturer	Shaft	Stiffness Rating	Manufacturer	Shaft	Stiffness Rating	Manufacturer	Shaft	Stiffness Rating
1	A1	Regular	2	I	Ladies	7	AH	Stiff
1	A2	Regular	2	J	Regular	8	AK	Stiff
1	A3	Regular	3	K1	Regular	9	AO	Stiff
1	A4	Regular	3	K2	Regular	10	AS	Stiff
1	B	Regular	3	K3	Regular	11	AV	Ladies
1	C1	Regular	3	K4	Regular	12	AY	Ladies
1	C2	Regular	3	L1	Ladies	13	BE	Ladies
1	C3	Regular	3	L2	Ladies	14	BH1	Regular
1	D1	Stiff	3	M1	Ladies	14	BH2	Regular
1	D2	Stiff	3	M2	Ladies	14	BH3	Regular
1	E1	Regular	3	AU1	Regular	14	BI1	Ladies
1	E2	Regular	3	AU2	Regular	14	BI2	Ladies
1	E3	Regular	4	P	Stiff	14	BJ	Stiff
1	F1	Regular	5	R	Stiff	14	BK1	Regular
1	F2	Regular	5	T	Ladies	14	BK2	Regular
1	F3	Regular	6	AB	Ladies			
1	F4	Regular	7	AD	Ladies			
1	G1	Ladies	7	AE	Ladies			
1	G2	Ladies	7	AF1	Stiff			
1	G3	Ladies	7	AF2	Stiff			
1	G4	Ladies	7	AG	Regular			

Table 6.2. Shaft length data.

Manufacturer	Shaft	Length (m)	Manufacturer	Shaft	Length (m)	Manufacturer	Shaft	Length (m)	Manufacturer	Shaft	Length (m)
1	A1	1.111	1	F3	0.991	3	M2	1.064	10	AS	1.121
1	A2	1.117	1	F4	0.991	3	AU1	1.100	11	AV	1.086
1	A3	1.116	1	G1	0.964	3	AU2	1.089	12	AY	0.896
1	A4	1.117	1	G2	0.946	4	P	1.128	13	BE	1.094
1	B	1.116	1	G3	0.946	5	R	1.092	14	BH1	1.112
1	C1	1.116	1	G4	0.947	5	T	1.062	14	BH2	1.112
1	C2	1.109	2	I	1.079	6	AB	1.065	14	BH3	1.112
1	C3	1.112	2	J	1.089	7	AD	1.053	14	BI1	1.083
1	D1	1.112	3	K1	1.115	7	AE	0.986	14	BI2	1.082
1	D2	1.109	3	K2	1.115	7	AF1	1.126	14	BJ	1.124
1	E1	1.109	3	K3	1.115	7	AF2	1.129	14	BK1	1.126
1	E2	1.109	3	K4	1.115	7	AG	1.075	14	BK2	1.123
1	E3	1.109	3	L1	1.086	7	AH	1.026			
1	F1	0.972	3	L2	1.086	8	AK	1.122			
1	F2	0.972	3	M1	1.064	9	AO	1.111			

Table 6.3. Shaft mass data.

Manufacturer	Shaft	Mass (g)	Manufacturer	Shaft	Mass (g)	Manufacturer	Shaft	Mass (g)	Manufacturer	Shaft	Mass (g)
1	A1	65.24	1	F3	58.61	3	M2	66.85	10	AS	68.92
1	A2	64.02	1	F4	58.87	3	AU1	68.57	11	AV	63.11
1	A3	64.47	1	G1	53.61	3	AU2	76.95	12	AY	48.65
1	A4	62.82	1	G2	52.76	4	P	60.42	13	BE	53.44
1	B	68.73	1	G3	54.32	5	R	68.86	14	BH1	68.53
1	C1	63.71	1	G4	52.6	5	T	57.39	14	BH2	66.69
1	C2	64.39	2	I	71.09	6	AB	50.52	14	BH3	67.41
1	C3	62.2	2	J	72.16	7	AD	54.84	14	BI1	69.03
1	D1	62.27	3	K1	107.95	7	AE	60.34	14	BI2	72.49
1	D2	61.66	3	K2	101.49	7	AF1	72.88	14	BJ	69.42
1	E1	67.38	3	K3	96.27	7	AF2	65.38	14	BK1	70.73
1	E2	65.62	3	K4	100.53	7	AG	59.27	14	BK2	55.92
1	E3	62.39	3	L1	97.05	7	AH	66.54			
1	F1	55.7	3	L2	90.56	8	AK	74.93			
1	F2	56.81	3	M1	65.39	9	AO	71.3			

Table 6.4. Shaft wall thickness data

Manufacturer	Shaft	Thickness (mm)	Manufacturer	Shaft	Thickness (mm)	Manufacturer	Shaft	Thickness (mm)	Manufacturer	Shaft	Thickness (mm)
1	A1	0.883	1	F3	0.88	3	M2	1.112	10	AS	0.898
1	A2	0.859	1	F4	0.892	3	AU1	1.087	11	AV	0.871
1	A3	0.851	1	G1	0.751	3	AU2	1.185	12	AY	0.841
1	A4	0.882	1	G2	0.777	4	P	0.712	13	BE	0.652
1	B	1.023	1	G3	0.766	5	R	0.703	14	BH1	0.869
1	C1	0.936	1	G4	0.778	5	T	0.754	14	BH2	0.894
1	C2	0.971	2	I	1.022	6	AB	0.564	14	BH3	0.884
1	C3	0.944	2	J	1.084	7	AD	0.825	14	BI1	0.794
1	D1	0.939	3	K1	1.438	7	AE	0.991	14	BI2	0.829
1	D2	0.979	3	K2	1.463	7	AF1	0.962	14	BJ	0.921
1	E1	0.977	3	K3	1.443	7	AF2	0.971	14	BK1	0.94
1	E2	0.981	3	K4	1.483	7	AG	0.905	14	BK2	0.888
1	E3	0.948	3	L1	1.228	7	AH	1.094			
1	F1	0.926	3	L2	1.218	8	AK	1.068			
1	F2	0.9	3	M1	1.104	9	AO	0.979			

Table 6.5. Shaft stiffness data for single cantilever length (800 mm)

Manufacturer	Shaft	Stiffness (N/m)	Manufacturer	Shaft	Stiffness (N/m)	Manufacturer	Shaft	Stiffness (N/m)	Manufacturer	Shaft	Stiffness (N/m)
1.0	A1	235.6	1.0	F3	260.1	3.0	M2	190.8	10.0	AS	265.6
1.0	A2	223.2	1.0	F4	267.3	3.0	AU1	209.2	11.0	AV	184.2
1.0	A3	219.4	1.0	G1	226.4	3.0	AU2	238.7	12.0	AY	180.8
1.0	A4	225.6	1.0	G2	218.0	4.0	P	209.2	13.0	BE	210.8
1.0	B	233.2	1.0	G3	204.2	5.0	R	284.5	14.0	BH1	224.4
1.0	C1	222.4	1.0	G4	212.1	5.0	T	210.9	14.0	BH2	241.0
1.0	C2	227.0	2.0	I	262.3	6.0	AB	131.8	14.0	BH3	249.2
1.0	C3	219.2	2.0	J	284.6	7.0	AD	198.4	14.0	BI1	191.0
1.0	D1	242.6	3.0	K1	197.0	7.0	AE	201.7	14.0	BI2	280.0
1.0	D2	253.7	3.0	K2	217.2	7.0	AF1	264.3	14.0	BJ	273.5
1.0	E1	211.6	3.0	K3	203.9	7.0	AF2	267.0	14.0	BK1	234.4
1.0	E2	214.7	3.0	K4	209.4	7.0	AG	221.9	14.0	BK2	231.9
1.0	E3	215.0	3.0	L1	215.6	7.0	AH	246.5			
1.0	F1	264.1	3.0	L2	199.6	8.0	AK	243.4			
1.0	F2	276.2	3.0	M1	188.9	9.0	AO	268.9			

Table 6.6. Shaft stiffness data for variable cantilever length (L-150 mm).

Manufacturer	Shaft	Stiffness (N/m)	Manufacturer	Shaft	Stiffness (N/m)	Manufacturer	Shaft	Stiffness (N/m)	Manufacturer	Shaft	Stiffness (N/m)
1.0	A1	161.8	1.0	F3	245.8	3.0	M2	146.9	10.0	AS	176.1
1.0	A2	152.5	1.0	F4	241.9	3.0	AU1	156.5	11.0	AV	127.8
1.0	A3	147.5	1.0	G1	224.5	3.0	AU2	175.5	12.0	AY	218.0
1.0	A4	157.2	1.0	G2	227.4	4.0	P	147.5	13.0	BE	161.1
1.0	B	154.6	1.0	G3	201.9	5.0	R	191.1	14.0	BH1	151.6
1.0	C1	159.7	1.0	G4	219.4	5.0	T	161.1	14.0	BH2	158.4
1.0	C2	161.3	2.0	I	195.1	6.0	AB	104.7	14.0	BH3	169.9
1.0	C3	157.2	2.0	J	215.4	7.0	AD	158.5	14.0	BI1	137.9
1.0	D1	172.6	3.0	K1	143.6	7.0	AE	195.7	14.0	BI2	194.1
1.0	D2	170.7	3.0	K2	155.9	7.0	AF1	171.1	14.0	BJ	175.5
1.0	E1	15.9	3.0	K3	140.6	7.0	AF2	173.7	14.0	BK1	159.3
1.0	E2	159.6	3.0	K4	148.4	7.0	AG	207.5	14.0	BK2	157.8
1.0	E3	161.4	3.0	L1	158.3	7.0	AH	217.5			
1.0	F1	255.3	3.0	L2	143.8	8.0	AK	164.9			
1.0	F2	269.6	3.0	M1	147.9	9.0	AO	201.1			

Table 6.7. Kickpoint data for shafts as a single cantilever length (800 mm).

Shaft	Kickpoint (%)	Shaft	Kickpoint (%)	Shaft	Kickpoint (%)	Shaft	Kickpoint (%)
A1	51.5	F3	51.1	M2	51.6	AS	47.5
A2	52.0	F4	51.2	AU1	48.4	AV	47.3
A3	50.9	G1	51.5	AU2	48.1	AY	49.1
A4	50.9	G2	52.0	P	48.1	BE	53.0
B	52.9	G3	50.9	R	48.2	BH1	47.0
C1	51.3	G4	50.9	T	53.1	BH2	47.1
C2	51.1	I	52.9	AB	51.9	BH3	47.2
C3	50.7	J	51.7	AD	52.1	BI1	49.8
D1	51.2	K1	50.4	AE	52.2	BI2	49.1
D2	50.1	K2	49.6	AF1	52.4	BJ	46.8
E1	52.4	K3	50.4	AF2	52.0	BK1	46.5
E2	51.9	K4	49.4	AG	49.2	BK2	46.9
E3	52.7	L1	50.7	AH	50.2		
F1	51.4	L2	50.6	AK	48.7		
F2	51.4	M1	51.5	AO	48.1		

Table 6.8. Kickpoint data for shafts at a variable cantilever length (L - 150 mm).

Shaft	Kickpoint (%)	Shaft	Kickpoint (%)	Shaft	Kickpoint (%)	Shaft	Kickpoint (%)
A1	51.4	F3	49.9	M2	50.3	AS	47.1
A2	51.5	F4	51.0	AU1	47.6	AV	47.8
A3	51.2	G1	51.4	AU2	47.2	AY	48.3
A4	51.0	G2	51.5	P	45.0	BE	52.2
B	51.9	G3	51.2	R	47.6	BH1	46.5
C1	50.6	G4	51.0	T	51.8	BH2	46.4
C2	50.5	I	52.5	AB	52.1	BH3	46.7
C3	50.5	J	51.1	AD	51.4	BI1	47.1
D1	50.7	K1	51.3	AE	51.7	BI2	47.6
D2	50.5	K2	49.4	AF1	51.5	BJ	45.9
E1	51.5	K3	50.1	AF2	51.2	BK1	45.8
E2	51.6	K4	49.6	AG	48.8	BK2	46.1
E3	51.5	L1	50.1	AH	49.1		
F1	51.1	L2	49.6	AK	47.5		
F2	51.3	M1	50.6	AO	48.4		

References

- Ashby, M. F. (1999). Materials selection in mechanical design, 2nd ed (pp. 376 - 405), Butterworth Heinemann, London.
- Betzler, N. F. (2010). The Effect of Differing Shaft Dynamics on the Biomechanics of the Golf Swing. PhD thesis, Edinburgh Napier University.
- Betzler, N. F., Slater, C., Strangwood, M., Monk, A., Otto, S., & Wallace, E. (2011). The Static and dynamic stiffness behaviour of composite golf shafts and their constituent materials. Sports Engineering, 14 (1), 27 – 37.
- Brouillette, M. (2002). On measuring the flexural rigidity distribution of golf shafts. In E. Thain (Ed.), Science and Golf IV: Proceedings of the World Scientific Congress of Golf (pp. 387-401). London: Routledge.
- Butler, J. H., & Winfield, D. (1994). The dynamic performance of the golf shaft during the downswing. In: A. .J. Cochran, M. R. Farrally. Science and Golf II: Proceedings of the world scientific congress of golf (pp. 259 – 264), 1st eden. E & F Spon, London, UK.
- Butler, J. H., & Winfield, D. (1995). What shaft is best for you? In A. J. Cochran (Ed.), Golf - the scientific way (pp. 113-115). Hemel Hempstead: Aston.
- Chen, C., Inoue, Y., & Shibata, K. (2005). Study on the interaction between human arms and golf clubs in the golf downswing. In A. Subic & S. Ujihashi (Eds.), The impact of technology on sport (pp. 175-180). Melbourne: Australasian technology Alliance.
- Cheong, S. K., Kang, K. W., et al. (2005). Evaluation of the mechanical performance of golf shafts. Engineering Failure Analysis.

- Chou, A., & Roberts, O. C. (1994). Golf shaft flex point - an analysis of measurement techniques. In A. J. Cochran & M. R. Farrally (Eds.), Science and golf II (pp. 278-283). London: E & FN Spon
- Gilat, A., Goldberg, R. K. & Roberts, G.D. (2002). Experimental study of strain-rate dependent behaviour of carbon/epoxy composite. Composite Science and Technology. 1469 -1476.
- Horwood, G. P. (1994). Golf shafts - a technical perspective. In A. J. Cochran & M. R. Farrally (Eds.), Science and Golf II (pp. 247-258). London: E & FN Spon.
- Horwood, G. (1994). Flexes, bend points and torques. Golf The Scientific Way. A.J. Cochran, Aston Publishing Group: 103-115.
- Howell, D. D. (1992). The Design of Filament Wound Graphite/Epoxy Golf Shafts. In G. Grimes (Ed.), Materials Working for You in the 21st Century. 37th International SAMPE symposium (pp. 1392-1405). Anaheim: SAMPE.
- Hull, D. & Clyne, T. W. (1996), An Introduction to Composite Materials, 2nd ed, Cambridge University Press, Cambridge.
- Huntley, M. P. (2007). Comparison of Static and Dynamic Carbon Fibre Composite Golf Club Shaft Properties and their Dependence on Structure. PhD thesis, University of Birmingham
- Huntley, M. P., Davis, C. L., Strangwood, M., & Otto, S. R. (2006). Comparison of the static and dynamic behaviour of carbon fibre composite golf club shafts. Proceedings of the Institution of Mechanical Engineers Part LJournal of Materials-Design and Applications, 220(L4), 229-236.
- MacKenzie, S. J. (2005). Understanding the role of shaft stiffness in the golf Swing. PhD Thesis, University of Saskatchewan.

- Mackenzie, S. J., & Sprigings, E. J. (2009). Understanding the role of shaft stiffness in the golf swing. Sport Engineering, 12, 13-19
- Maltby, R. D. (1995). Golf club design, fitting, alteration, and repair: the principles and procedures (Rev. 4th ed.). Newark, OH: R. Maltby Enterprises
- Mather, J. S. B., & Jowett, S. (2000). Three dimensional shape of the golf club during the swing. In A. Subic & S. Haake (Eds.), The Engineering of Sport (pp. 77-85). London: Blackwell Science.
- Matthews, F. L. And Rawlings, E. R. D. (1994). Composite materials: Engineering and science, Woodhead publishing limited.
- Milne, R. D. (1990). What is the role of the golf shaft in the golf swing? Science and golf. (pp. 252-257). E&FN SPON.
- Milne, R. D., & Davis, J. P. (1992). The role of the shaft in the golf swing. Journal of Biomechanics, 25(9), 975-983.
- Newman, S., Clay, S., & Strickland, P. (1997). The dynamic flexing of a golf club shaft during a typical swing. In Fourth Annual Conference on Mechatronics and Machine Vision in Practice, Proceedings (pp. 265-270).
- Painter, P. C. & Coleman, M. M. (2009). The Essentials of Polymer Science and Engineering. DEStech Publications.
- Penner, A. R. (2003). The physics of golf. Reports on Progress in Physics*, 66*(2), 131-171.
- Stanbridge, K., Jones, R., & Mitchell, S. (2004). The effect of shaft flexibility on junior golfers' performance. Journal of Sports Sciences, 22(5), 457-464.
- Strangwood, M. (2003). PGA Technical Manual. PGA, The Belfry.
- Summitt, J. (2000). The modern guide to shaft fitting. Dynacraft. Ohio.

- Tsujiuchi, N., Koizumi, T., & Tomii, Y. (2002). Analysis of the influence of golf club design on the golf swing. In S. Ujihashi & S. Haake (Eds.), The Engineering of Sport 4 (pp. 537-544). Oxford: Blackwell.
- Wallace, E. S., & Hubbell, J. E. (2001). The effect of golf club shaft stiffness on golf performance variables - implications for club-fitting. Paper presented at the Materials & Science in Sports Symposium, Coronado Island Marriott Resort, Coronado, California.
- Wallace, E. S., Otto, S. R., & Nevill, A. (2007). Ball launch conditions for skilled golfers using drivers of different lengths in an indoor testing facility. Journal of Sports Sciences, 25(7), 731 - 737.
- Werner, F. D. and Greig, R. C. (2001). Behaviour of golf club shafts. How golf clubs really work and how to optimise their design, Origin Inc.
- Worobets, J. T., & Stefanyshyn, D. J. (2008). Shaft stiffness: implications for club fitting. In D. J. Crews & R. Lutz (Eds.), Science and Golf V (pp. 431- 437). Mesa, AZ: Energy in Motion.